

IMPROVEMENT OF SHORT-RANGE DISPERSION MODELS TO ESTIMATE THE AIR QUALITY IMPACT OF POWER PLANTS IN URBAN ENVIRONMENTS

Prepared For:

California Energy Commission
Public Interest Energy Research
Program

In Collaboration With:

California Environmental Protection Agency

 **Air Resources Board**



Arnold Schwarzenegger
Governor

PIER COLLABORATIVE REPORT

December 2008
CEC-500-2007-096

Prepared By:

Akula Venkatram
Department of Mechanical Engineering
University of California, Riverside
Riverside, California 92521
Commission Contract No. 500-01-038

California Air Resources Board

Tony Servin

Project Manager

Prepared For:

Public Interest Energy Research (PIER)

California Energy Commission

Marla Mueller

Project Manager

Marla Mueller

Contract Manager

Linda Spiegel

Program Area Lead

Energy-Related Environmental Research

Mike Gravely

Office Manager

Energy Systems Research



Martha Krebs, Ph.D

PIER Director

Thom Kelly, Ph.D.

Deputy Director

ENERGY RESEARCH & DEVELOPMENT DIVISION

Melissa Jones

Executive Director

DISCLAIMER

This report was prepared as the result of work sponsored by the California Energy Commission. It does not necessarily represent the views of the Energy Commission, its employees or the State of California. The Energy Commission, the State of California, its employees, contractors and subcontractors make no warrant, express or implied, and assume no legal liability for the information in this report; nor does any party represent that the uses of this information will not infringe upon privately owned rights. This report has not been approved or disapproved by the California Energy Commission nor has the California Energy Commission passed upon the accuracy or adequacy of the information in this report.

Acknowledgments

The project team from the University of California, Riverside (UCR), consisted of David Pankratz, Jing Yuan, Tao Zhan, and Sang-Mi Lee. Professor Marko Princevac and his students were responsible for the meteorological measurements made during the 2005 fields study in Wilmington. A large number of undergraduate students from UCR played a critical role in conducting the field study and in processing the resulting data. Sally Pedersen and James Bristow led this group of students. Graduate students Wenjun Qian and Gokul Krishnan helped analyze the data from the 2005 study and helped prepare the final report. Dr. Ashok Luhar from Australia's Commonwealth Scientific and Industrial Research Organization (CSIRO) played a critical role in developing methods to estimate urban micrometeorology from rural measurements.

The project members thank Vlad Isakov (now at the U.S. Environmental Protection Agency) for helping with the study design, data analysis, and modeling related to the 2003 and 2004 Wilmington field studies.

This report was submitted in fulfillment of ARB Contract Number 00-720, "Development of Dispersion Models to Estimate Air Toxics Risk in Urban Environments," under the sponsorship of Energy Commission and ARB. Work was completed as of September 6, 2006. The ARB and the Energy Commission initiated a program in 2001 at UC Riverside (Contract No: 3900-001-0044, Energy Commission Project Number 500-01-038).

Disclaimer

The statements and conclusions in the report are those of the contractor and not necessarily those of the California Air Resources Board. The mention of commercial products, their source, or their use in connection with material reported herein is not to be construed as actual or implied endorsement of such products.

Please cite this report as follows:

Venkatram, Akula. 2008. *Improvement of Short-Range Dispersion Models to Estimate Air Quality Impact of Power Plants in Urban Environments*. California Energy Commission, PIER Energy-Related Environmental Research Program. CEC-500-2007-096.

Preface

The California Energy Commission's Public Interest Energy Research (PIER) Program supports public interest energy research and development that will help improve the quality of life in California by bringing environmentally safe, affordable, and reliable energy services and products to the marketplace.

The PIER Program conducts public interest research, development, and demonstration (RD&D) projects to benefit California.

The PIER Program strives to conduct the most promising public interest energy research by partnering with RD&D entities, including individuals, businesses, utilities, and public or private research institutions.

PIER funding efforts are focused on the following RD&D program areas:

- Buildings End-Use Energy Efficiency
- Energy Innovations Small Grants
- Energy-Related Environmental Research
- Energy Systems Integration
- Environmentally Preferred Advanced Generation
- Industrial/Agricultural/Water End-Use Energy Efficiency
- Renewable Energy Technologies
- Transportation

Improvement of Short-Range Dispersion Models to Estimate Air Quality of Power Plants in Urban Environments is the final report for the Short Range Dispersion Study project (Contract Number 500-01-038) conducted by the University of California, Riverside. The information from this project contributes to PIER's Energy-Related Environmental Research Program.

For more information about the PIER Program, please visit the Energy Commission's website at www.energy.ca.gov/pier or contact the Energy Commission at 916-654-5164.

Table of Contents

Preface.....	iii
Abstract	ix
Executive Summary	1
1.0 Introduction.....	9
1.1. Motivation for Project and Purpose of Report	9
1.2. Report Structure	11
2.0 Wilmington Field Studies and Dispersion Models for Shoreline Releases	13
2.1. Introduction	13
2.2. Wilmington 2004 Study	13
2.2.1. Concentration and Meteorological Measurements	13
Tracer Concentration Measurements	13
Meteorological Measurements	15
2.2.2. Characteristics of Meteorological Variables	16
2.2.3. Dispersion Parameters	20
2.2.4. Analysis of Concentrations.....	23
2.3. Wilmington 2005 Study	28
2.3.1. Experimental Design and Implementation	28
2.3.2. Modeling	30
Model Formulation	30
Model Evaluation	34
2.4. Conclusions	38
2.5. Modifications to AERMOD Interface	39
3.0 References.....	45
4.0 Glossary	49

Appendix A	Measurement Report for Technical Support Study of the Wilmington Field Study
Appendix B	Tracer Release System Failure
Appendix C	Measurements and Data Processing for the Wilmington 2004 Field Study
Appendix D	Quality Assurance Audit Report for the Wilmington 2004 Field Study
Appendix E	Wind Data Summary and Wind Roses for the Wilmington 2004 Field Study
Appendix F	Tracer Release and Sampling Details for the Wilmington 2004 Field Study

Appendix G	Measurements and Data Processing for the Wilmington 2005 Field Study
Appendix H	Quality Assurance Audit Report for the Wilmington 2005 Field Study
Appendix I	Key to Electronic Data Files
Appendix J	Estimating Micrometeorological Inputs for Modeling Dispersion in Urban Areas During Stable Conditions

List of Figures

Figure 2.1. Map of study area and equipment locations for Wilmington 2004 study.....	14
Figure 2.2. Comparison of surface friction velocities and heat fluxes measured by sonic anemometers at LADWP (release site) and JWPCP (downwind site) on 9/3/2004 and 9/9/2004.....	16
Figure 2.3. Profiles of potential temperatures measured on 9/3/2004 at downwind site.....	18
Figure 2.4. Meteorological profiles observed on hour 7 on 9/3/2004 at the release site. Vertical lines represent mean values of the variables.....	19
Figure 2.5. Variation of turbulent intensities and transport wind speeds used in the dispersion model for Wilmington 2004 study. Horizontal lines correspond to mean values of the variables.....	20
Figure 2.6. Crosswind concentration profiles measured on 9/2/2004 at 11:00. Arcs 1 through 5 are 100 m, 400 m, 1000 m, 3000 m, and 5000 m from source, respectively.	21
Figure 2.7. The variation of dispersion parameters as a function of downwind distance for the Wilmington 2004 study. The solid straight lines represent linear growth determined by the mean turbulent intensities.	22
Figure 2.8. Comparison of measured horizontal plume spreads with model estimates during the (a) first six days and (b) last two days of the Wilmington 2004 study	23
Figure 2.9. The variation of observed arc maximum concentrations with downwind distance for the Wilmington 2004 study.....	24
Figure 2.10. Variation of the TIBL height at 5000 m during Wilmington 2004 study	27
Figure 2.11. Comparison of measured arc maximum concentrations with model estimates during the first six days (upper panels) and the last two days (lower panels) of Wilmington 2004 study. Right panels correspond to modifications described in the text.	28
Figure 2.12. Map of study area and equipment locations for the Wilmington 2005 study	30
Figure 2.13. The variation of observed arc maximum concentrations with downwind distance for releases into stack and below stack top for the Wilmington 2005 study	31
Figure 2.14. Entrainment of plume by growing internal boundary layer.....	31
Figure 2.15. Variation of meteorological inputs used to model buoyant releases on 6/27/2005. Case numbers 1 through 5 correspond to hours 7 through 11.	35
Figure 2.16. Comparison of measured arc maximum concentrations with model results for in-stack releases for the Wilmington 2005 study.....	36

Figure 2.17. Comparison of measured arc maximum concentrations with model results for in-stack releases for the Wilmington 2005 study. $L_y = 1000$ m in Equation (2.4) for horizontal spread.	36
Figure 2.18. Variation of meteorological inputs used to model below stack top releases for the Wilmington 2005 study. Case numbers 1 through 4 correspond to hours 8 through 11 of June 26, while case numbers 5 through 9 refer to hours 7 through 11 of June 28.....	37
Figure 2.19. Comparison of measured arc maximum concentrations with model results for below stack top releases for the Wilmington 2005 study	38
Figure 2.20. Comparison of estimated surface friction velocities and heat fluxes with observations made at LADWP site for the Wilmington 2004 study. The lines above and below the one-to-one correspond to a factor of two interval.....	41
Figure 2.21. Comparison of estimated surface and 50 m (boundary layer, BL) turbulence levels with observations made at the LADWP site for the Wilmington 2004 study. The lines above and below the one-to-one correspond to a factor of two interval.	41
Figure 2.22. Comparison of model results with arc maximum concentrations measured during the 2004 Wilmington field study.....	42
Figure 2.23. Comparison of measured arc maximum concentrations with model results for in-stack releases for the Wilmington 2005 study. Meteorological inputs estimated from 50 m wind speed and Equation (2.30). $L_y = 1000$ m in Equation (2.4) for horizontal spread.....	43
Figure 2.24. Comparison of measured arc maximum concentrations with model results for below stack top releases for the Wilmington 2005 study. Meteorological inputs estimated from 50 m wind speed and Equation (2.30).	43

Abstract

As California moves to a more diverse electricity supply portfolio, from primarily central power plants to include more distributed generation, it is important to understand and estimate reliably the near-source toxic exposure rates from both existing and potential generation sources. Therefore, the California Energy Commission and the California Air Resources Board sponsored the University of California at Riverside to conduct field studies and create near-field urban shoreline dispersion models. At the Los Angeles Department of Water & Power electric plant in Wilmington, researchers released tracer gases at ground level, three meters below the 67-meter stack height, and with the exhaust gases in the stack. Sulfur hexafluoride (SF₆) tracer was sampled with fixed ground-level bag-samplers at downwind distances from 100 meters to 5 kilometers. These studies determined that current models are inadequate for near-field urban shoreline dispersion modeling. Measurements of surface and aloft winds and sulfur hexafluoride concentration measurements were used to develop and evaluate models that can describe dispersion of shoreline releases at heights ranging from ground level to 300 meters. The effort has resulted in improvement and verification of existing dispersion models used for regulatory purposes in the United States.

Keywords: Near-field urban shoreline dispersion modeling, tracer, power generation emissions dispersion, Wilmington, air toxics

Executive Summary

Background

It is important to understand and reliably estimate the toxic exposure and changes in toxic exposure that may be occurring very close to the source in urban areas that have or may be siting power generation sources as California moves to a more diverse electricity supply portfolio. The atmospheric dispersion modeling system American Meteorological Society/Environmental Protection Agency Regulatory Model, AERMOD, is used to predict if there may be adverse impacts from siting a new source. However, AERMOD is not designed to estimate the nearby air quality impact of such urban and shoreline sources. Therefore, the California Energy Commission (Energy Commission) and the California Air Resources Board (ARB) sponsored the University of California at Riverside to improve short-range dispersion models that can be used to estimate the air quality impact of emissions from urban sources, including central power plants and distributed generation plants, located on California shorelines. A field study was used to improve dispersion models for incorporation into AERMOD. The field study measured the meteorological parameters (for example, wind speed and direction, heat flux) as well as how the exhaust plume dispersed from the stack to ground level. This data was used to evaluate the performance of short-range dispersion models in urban areas.

Methods

The dispersion models were developed, evaluated, and improved with tracer and meteorological data collected in field studies at the Los Angeles Department of Water & Power power plant in Wilmington. The studies were conducted in three phases. The first phase, conducted in September 2003, was a technical support study to obtain information on wind speed and direction and determine where to locate the ground level monitors for the second and third phases. Phase Two was conducted from August 24 to September 11, 2004, and consisted of eight daytime experiments. Although this study was designed to provide data on dispersion from elevated releases, a leak in the release system resulted in near-surface releases at the foot of the power plant during the entire second phase of experiments. Therefore, a third phase was conducted from June 9-30, 2005, where the leak was repaired and four elevated releases—two non-heated elevated releases and two “in-stack” releases to measure the hot power plant plume—were successfully conducted. During each experiment, the invisible, inert tracer gas sulfur hexafluoride was released and then measured downwind at 70 fixed monitoring locations. The sulfur hexafluoride gas has the same buoyancy as the exhaust gases and so behaves like a pollutant in the exhaust, effectively acting like a “tracer” for where the exhaust plume travels. In addition to the fixed monitoring locations, a van-based mobile platform was outfitted with real-time sulfur hexafluoride monitoring instruments to track the plume. Measurements of surface winds and winds aloft (up to approximately one kilometer above ground) were made throughout the experiment.

Results

This project has resulted in two unique databases of dispersion from shoreline urban sources at distances ranging from 100 to 5000 meters (m) from the source. The data has been used to develop and validate new dispersion models that can be used to estimate toxic ground-level concentrations from shoreline power generation where the stack of the power plant ranges from near ground-level (corresponding to a smaller distributed generation unit) to about 300 m high (corresponding to the height the exhaust gases of the Los Angeles Department of Water & Power power plant in Wilmington). The models incorporate the unique meteorological effects of shoreline locations. The modeled versus measured results compared well and indicated that the new model can successfully predict shoreline effects.

The research team has also developed a meteorological processor that converts normally available meteorological data (wind speed and direction) into the more detailed meteorological inputs required by the models. The team has performed a preliminary evaluation of the method using the Wilmington data sets.

The major features of the shoreline dispersion model and the associated meteorological processor have been designed for incorporation into AERMOD, the U.S. Environmental Protection Agency's (U.S. EPA's) regulatory model for short-range applications.

Conclusions

This study's major conclusions are:

- The lower atmosphere has a natural lid, or "boundary layer" that inhibits vertical mixing beyond the lid. This prevents air from rising above the top of the layer, and preventing air in the upper atmosphere from moving downward into the lower layer. The boundary layer height begins at approximately 100 m high at the shoreline and increases to 500 m as it moves inland. The elevated plume travels above the lower layer for several hundred meters. Thus the pollutants from the plume are not detected at ground-level until it has traveled approximately one kilometer from the stack.
- At 100 meters, the concentrations from ground level releases can be an order of magnitude larger than seen at any distance from the elevated releases (power plants). However, at distances beyond 1000 m, the concentrations look very similar for ground and elevated releases. Concentrations from ground-level releases decrease with downwind distance roughly an order of magnitude from 100 to 500 m and another order of magnitude at 1000 m. Currently used models for the growth of the thermal internal boundary layer underestimate the extent of vertical mixing inferred from ground-level concentration observations. Thus current models may underestimate the air quality impacts from ground-level sources near the shore. This study provides the first data sets to try to better understand the physical processes that govern the thermal internal boundary layer on California shorelines.
- The data indicate that it is necessary to account for building-induced vertical spread when the release is close to a building. This conclusion confirms results from other

similar studies. Lateral spread is also likely to be enhanced by buildings, but results from this study were not sensitive to the inclusion of initial horizontal spread.

- Simple dispersion models can be developed to simulate the dispersion of both surface and elevated shoreline sources in urban areas. The meteorological inputs for these models consist of measurements of boundary layer variables at a height of 50 m. This height corresponds to the well-mixed region of the thermal internal boundary layer, which ranges in height from 100 m close to the source to more than 500 m at 5 kilometers (km) from the source.

Recommendations

The field studies conducted in this project have resulted in a database that contains invaluable information on dispersion and the associated meteorology in coastal urban areas. Only a small fraction of this database has been analyzed to obtain the results presented in this report. The research team recommends further analysis of the data to resolve uncertainties in the dispersion model and obtain more understanding of the meteorology.

The dispersion and meteorological models described in this report need to be evaluated with databases that are independent of the Wilmington databases used to develop them. The research team recommends testing them with data from similar field studies such as the Nanticoke Shoreline Diffusion Experiment and the Kwinana Coastal Fumigation Study.

The research team recommends that the major features of the shoreline dispersion models described in this report be incorporated in current regulatory models to allow its application to an important class of sources. The research team is participating on the U.S. EPA panel to incorporate these improvements.

Benefits to California

This research provided test data of a typical shore-side California power plant and improved understanding of the toxic impact to nearby residents, resulting in some of the first-of-its-kind detailed information on how the exhaust plume disperses into the nearby community under different weather conditions. The official regulatory model of the U.S. EPA for estimating near-source dispersion impacts has been updated to reflect this new information. This has resulted in the ability to better determine impacts from power generation emissions in urban areas in California, and to better determine whether emissions from a proposed power generation unit could present an undue risk to populations in adjacent areas.

Technical Executive Summary

Background

As California moves to a more diverse electricity supply portfolio it is important to understand and estimate reliably the near-source toxic exposure rates from both existing and potential generation sources. Because the currently used atmospheric dispersion model, AERMOD, is not designed to estimate the air quality impact of such sources, the California Energy Commission (Energy Commission) and the California Air Resources Board (ARB) sponsored the University of California at Riverside to develop short-range dispersion models that can be used to estimate the air quality impact of emissions from urban sources, including power plants, located on California shorelines. The meteorological inputs (for example, wind speed and direction, heat flux) for these models are designed to be compatible with those used in AERMOD, to allow incorporation of the dispersion models into AERMOD. These models, applicable to source-receptor distances of kilometers (km), were evaluated with data from two field studies. The second objective of the project is to compile and organize the data collected in these field studies to extend the databases for evaluating the performance of short-range dispersion models in urban areas.

Methods

The dispersion models were developed, evaluated, and improved with tracer and meteorological data collected in field studies conducted near the Los Angeles Department of Water & Power (LADWP) power plant in Wilmington. The studies were conducted in three phases. The first phase, conducted in September 2003, was a technical support study to obtain information on (a) the magnitude and range of tracer concentrations in the area during a field experiment, (b) the meteorology in the area, and (c) the locations for fixed monitoring sites.

The data from the technical support study were used to design the second phase, which was conducted during August 24 to September 11, 2004. Sulfur hexafluoride (SF₆) tracer gas was released during eight daytime experiments, each lasting two to six hours. Although this study was designed to provide data on dispersion from elevated buoyant releases, a leak in the release system resulted in near surface releases at the foot of the power plant during the entire second phase of experiments.

The third phase of the study, conducted from June 9 to 30, 2005, included four daytime experiments. Each experiment lasted approximately four hours. In two of these experiments, SF₆ was introduced into the power plant stack at a location that allowed for complete mixing and temperature equilibration with the stack gases before being emitted from the stack. During the other two experiments, the tracer gas was released approximately 3 meters (m) below the top of the 67 m-tall power plant stack.

During each study, the dispersed SF₆ was monitored at ground level using 60-72 fixed-location integrated bag-samplers downwind from the plant and one van-based mobile platform, which was outfitted with real-time SF₆ monitoring instrumentation. Measurements of surface winds

and winds aloft (up to approximately one kilometer) were made using a combination of sonic anemometers and remote-sensing acoustic sodars.

Results

The research team has developed new dispersion models that can be used to estimate ground-level concentrations associated with shoreline releases at heights ranging from near ground-level to about 300 m, corresponding to the plume height of the buoyant gases of the LADWP power plant in Wilmington. The models incorporate the growing internal boundary that forms when stable air from the ocean flows onto the warmer urban surface. The model performance statistics are comparable or better than those reported in the literature for similar model development exercises.

This project has resulted in two unique databases relevant to dispersion from shoreline urban sources at source-receptor distances ranging from 100 m to 5000 m from the source.

The research team has also proposed a method to construct the meteorological inputs required by the dispersion models from routinely available surface and upper level observations. The team has performed a preliminary evaluation of the method using the Wilmington data sets.

The major features of the shoreline dispersion model and the associated meteorological processor have been designed for incorporation into AERMOD, the U.S. Environmental Protection Agency's (U.S. EPA's) regulatory model for short-range applications.

Conclusions

This study's major conclusions are:

- Concentrations at ground level from ground-level releases can be an order of magnitude larger than those seen for the elevated releases very near (100 m) to the source. However, at distances beyond 500 m the concentrations look very similar for ground and elevated releases. Concentrations from ground-level releases decrease with downwind distance roughly an order of magnitude from 100 to 500 m and another order of magnitude at 1000 m. Conversely, ground level concentrations for in-stack elevated releases increase with downwind distance. The lower atmosphere has a natural lid, or "boundary layer" that inhibits vertical mixing beyond the lid. This prevents air from rising above the top of the layer, and preventing air in the upper atmosphere from moving downward into the lower layer. The boundary layer height begins at approximately 100 m high at the shoreline and increases to 500 m as it moves inland. The presence of increasing downwind concentrations from the power plant indicates that as the boundary layer height increases, the plume, which was originally above the boundary layer near the shoreline starts to enter, into the lower atmosphere as it moves inland.
- The thermal internal boundary layer, which forms when stable air over water flows onto warmer land, plays a crucial role in governing concentrations caused by both surface and elevated releases near the shoreline. Ground-level concentrations associated with elevated emissions, such as those from power plants, are determined by the rate at

- Currently used models for the growth of the thermal internal boundary layer underestimate the extent of vertical mixing inferred from ground-level concentration observations. Although these models can be modified with measured data to explain an individual location there is a need for better understanding of the physical processes that govern the thermal internal boundary layer on California shorelines.
- The data indicate that it is necessary to account for building-induced vertical spread when the release is close to a building. This conclusion confirms results from other similar studies. Lateral spread is also likely to be enhanced by buildings, but results from this study were not sensitive to the inclusion of initial horizontal spread.
- Simple dispersion models can be developed to simulate the dispersion of both surface and elevated shoreline sources in urban areas. The meteorological inputs for these models consist of measurements of boundary layer variables at a height of 50 m. This height corresponds to the well-mixed region of the thermal internal boundary layer, which ranges in height from 100 m close to the source to more than 500 m at 5 km from the source.
- Preliminary evaluation of the method to construct meteorological model inputs from routinely available observations suggests that AERMET, AERMOD's meteorological processor, can be readily modified to account for shoreline thermal internal boundary layer effects.

Recommendations

The field studies conducted in this project have resulted in a database that contains invaluable information on dispersion and the associated meteorology in coastal urban areas. Only a small fraction of this database has been analyzed to obtain the results presented in this report. The research team recommends further analysis of the data to resolve uncertainties in the dispersion model and obtain more understanding of the meteorology. For example, it is necessary to understand the reasons for the discrepancy between model estimates of thermal internal boundary layer height and values inferred from measurements of temperature profiles. The unexpectedly large values of turbulence measured by the sodar above heights of 60 m need to be investigated.

The dispersion models and the meteorological processor described in this report need to be evaluated with databases that are independent of the Wilmington databases used to develop them. The research team recommends testing them with data from similar field studies such as the Nanticoke Shoreline Diffusion Experiment and the Kwinana Coastal Fumigation Study.

AERMOD was promulgated as the replacement for the Industrial Source Complex (ISC) model on November 9, 2005. At this stage, the model cannot be used to estimate the impact of shoreline sources because it does not contain formulations required to account for the

interaction between the shoreline thermal internal boundary layer and plumes from near-surface and elevated sources. The research team recommends that the major features of the shoreline dispersion models described in this report be incorporated in AERMOD to allow its application to an important class of sources.

The results presented here suggest that AERMET can be adapted for shoreline applications with relatively simple modifications to account for thermal internal boundary layer growth and the contribution of convective turbulence in the thermal internal boundary layer. The next step is to modify AERMOD and AERMET and evaluate them with the databases mentioned earlier. The research team is participating on the U.S. EPA panel to incorporate these improvements into AERMOD.

1.0 Introduction

1.1. Motivation for Project and Purpose of Report

Currently used short-range dispersion models, such as Industrial Source Complex (ISC) model or AERMOD, incorporate methods to treat urban dispersion, but these methods have undergone limited evaluation. For example, ISC uses empirical urban dispersion curves derived primarily from experiments conducted in a single city—St. Louis, Missouri—during 1963–1965 (McElroy and Pooler 1968). Their applicability to other cities has not been tested. Furthermore, these dispersion curves do not incorporate current understanding of relationships between micrometeorology and dispersion. AERMOD (Cimorelli et al. 2005) incorporates this understanding, but its ability to estimate dispersion in urban areas has been only evaluated with a single tracer data set collected around a highly buoyant release from a power plant stack located in Indianapolis (Murray and Bowne 1988). Until recently, there were little data that could be used to characterize dispersion in urban areas, especially for low-level sources at receptor distances of tens of meters to kilometers.

Recognizing the need for reliable data to characterize dispersion in urban areas, the California Resources Board (ARB) and the California Energy Commission (Energy Commission) initiated a program in 2001 at the University of California (UC) Riverside to conduct several tracer studies and use the data to develop dispersion models applicable to urban sources. The project has resulted in dispersion models that can be used to examine the impact of ground-level sources at source-receptor distances of the order of tens of meters to a few kilometers from near-ground sources (See Venkatram et al. 2005). These models can be incorporated into AERMOD in the future.

In 2003, Energy Commission extended the project to study dispersion from elevated power plant stacks located in coastal areas. The major objective of this phase of the project was to develop and evaluate dispersion models applicable to urban sources, including power plants, located in coastal areas. The second objective of the study was to develop a database that can be used by investigators involved in urban dispersion.

This study's researchers are aware of three major field studies that had goals similar to those of the current study. Cagnetti et al. (1988) describe a study conducted at a coastal site in Italy during June 1983 and 1984. In this study, sulfur hexafluoride (SF_6) was released at heights of 10 meters (m) and 50 m and sampled on arcs ranging from 1 kilometer (km) to 7 km from the release location. Tethersondes were used to measure winds, relative humidity, and pressure; and radiosondes were used to measure temperature profiles. Turbulent velocities or surface fluxes were not measured. Analysis of the ground-level concentrations yielded estimates of horizontal and vertical spreads, which were categorized using Pasquill stability classes. The major conclusion from this study is that the vertical spread of near surface releases is limited by the height of the thermal internal boundary layer (TIBL). Thus, estimating the height of the TIBL as function of distance from the shoreline is critical to modeling dispersion near shorelines. The results reported by Cagnetti et al. (1988) provide useful insight into dispersion but cannot be readily used to develop or evaluate dispersion models, especially for elevated

buoyant sources. It might be possible to interpret the concentrations observed in the Cagnetti study if the meteorological inputs required by the models described in this report can be inferred from the measurements made in the Cagnetti study.

Portelli (1982) describes a comprehensive field study (Nanticoke Shoreline Diffusion Experiment) conducted in the summers of 1978 and 1979 to understand dispersion of sulfur dioxide (SO₂) emissions from a 4000 MW power plant located on the north shore of Lake Erie. Mean winds and temperature in the boundary layer were measured using tether sondes and minisondes. The TIBL structure was characterized with information from tether sondes and acoustic sounders. The wind speeds and temperatures were also measured at two heights on a 85 m tower located 12 km inland. Surface heat and momentum fluxes were measured at a site about 7 km from the shoreline. Turbulent velocities in the boundary layer were measured using a sonic anemometer mounted on a kytoon, but were not reported until 1986 by Ogawa et al. (1986). Sulfur dioxide concentrations in the elevated plume, before it fumigated, were measured with helicopter traverses. Plume rise was measured using a Lidar. Ground-level concentrations at locations where the plume fumigated were measured using mobile monitors, which traversed the ground-level plume to obtain information on the horizontal extent of the plume. In addition, fixed measurements of SO₂ concentrations were made at 16 sites.

The Nanticoke Shoreline Diffusion Experiment resulted in one of the most comprehensive data sets available on this aspect of dispersion. It has been used by several authors (Misra and Onlock 1982; Kerman et al. 1982; Stunder and Sethuraman 1986) to develop and evaluate models for the growth of the TIBL and dispersion from elevated shoreline sources.

The most recent of the shoreline studies was conducted in Kwinana on the west coast of Australia between January 26 and February 6, 1995. Like the Nanticoke study, it was designed to understand fumigation of plumes from a power plant, the Kwinana Power Station. While the Kwinana study did not use as many instruments as the Nanticoke study, it filled a gap in the Nanticoke study by characterizing turbulence in the boundary layer using an instrumented aircraft. Data from the Kwinana study have been used by Luhar (1998, 2002) to develop and evaluate models for TIBL growth and shoreline dispersion.

The study described in this report differs from previous studies in that it was designed to understand dispersion in urban coastal areas, and estimate the relative ground-level impacts of near-surface and elevated sources at source-receptor distances of 100 m to several kilometers. The Nanticoke and Kwinana studies, conducted in rural areas, focused on fumigation at distances of tens of kilometers from large power plant sources. The current study combines some of the best features of the tracer study conducted by Cagnetti et al. (1988) and the power plant plume studies at Nanticoke and Kwinana. The use of tracers and an extensive sampling network, as in Cagnetti et al. (1988), allowed this study's researchers to map the ground-level plume and estimate the horizontal spread of the plume as a function of distance from the source. Like the Kwinana study, the research team measured turbulent velocities in the TIBL to relate the statistics of these velocities to plume spread. The team also measured surface heat and momentum fluxes to examine the relationship between these fluxes and the meteorology of the TIBL.

Tracer studies (Drivas and Shair 1974; Shair et al. 1982; Lamb et al. 1978a, 1978b) conducted in the Los Angeles area have examined transport and dispersion over spatial scales covering the entire Los Angeles Basin, and have been designed to understand the meteorological processes that govern photochemical smog. These studies provide few results that can be used to develop dispersion models for the kilometer scales considered in the current project. Thus, the study described in this report fills a gap in understanding of dispersion governed by the meteorology of the Los Angeles coastline.

This report describes the field studies and the models that resulted in fulfilling the objectives of the project.

1.2. Report Structure

The major objectives of the project were achieved by conducting tracer studies in the vicinity of the Los Angeles Department of Water & Power (LADWP) power plant in Wilmington, California. This study was conducted in three phases. The first phase, conducted in September 2003, was a technical support study (TSS) to obtain information on (a) the magnitude and range of tracer concentrations in the area during a field experiment, (b) the meteorology in the area, and (c) the locations for fixed monitoring sites.

The data from the TSS were used to design the second phase, conducted during August and September 2004. This study provided data on dispersion on near-surface releases in an urban area located on a shoreline. The data were used to develop a dispersion model applicable to such releases.

A third phase, conducted in June 2005, focused on elevated tracer releases. Two types of releases were used: non-buoyant releases 3 m below the top of the 67 m stack, and releases into the buoyant stack gases. The data from these experiments were used to develop new dispersion models.

The activities related to the second and third phases of the Wilmington field studies are summarized in Chapter 2 of this report. Appendix A describes activities and results from the TSS.

2.0 Wilmington Field Studies and Dispersion Models for Shoreline Releases

2.1. Introduction

The major objective of the Wilmington field studies sponsored by ARB and the Energy Commission was to formulate and evaluate short-range dispersion models for sources in coastal urban areas. The models were developed using data from field experiments conducted near the Harbor Generating Station of the LADWP in Wilmington, California. The power plant, which has a capacity of 224 MW, is housed in a building with a height of 40 m. Waste gases are exhausted through a stack with a height of 67 m and an inside diameter of 4.72 m. The gases exit at a velocity of 23 meters per second (m/s) and a temperature of 458 degrees kelvin (K). The plume buoyancy parameter works out to be $431 \text{ m}^4/\text{s}^3$, which results in a plume rise of about 175 m for the meteorological conditions observed during the field study.

Wilmington is a community of about 53,000 people located next to the Port of Los Angeles. It is surrounded by numerous small industries, transportation corridors, and port businesses, which are located to the south of residential areas. Figure 2.1 shows the map of Wilmington. The residential areas, consisting mostly of one-story buildings about 4 m high, are located downwind of the LADWP site during the dominant southwesterly flows. The building density is relatively low, suggesting flow in which wake interference is small.

Field studies were conducted in 2004 and 2005 in the Wilmington area. The first study, conducted during August and September 2004, was designed to study dispersion of buoyant releases from the power plant stack. After the study was completed, a preliminary analysis of the observed ground-level concentrations suggested that the SF_6 was not released from the stack. A subsequent investigation showed that there was a break in one of the polyethylene tubes used in the release system. A tube leaving the dilution air pump had melted and broken free from the exit point of the dilution air pump. The break resulted in most of the tracer gas leaving the tubing at the point of the break—at the surface—instead of going through the stack. This failure of equipment is discussed in more detail in Appendix B. Thus, the research team inadvertently obtained data for surface releases for all eight days of the study period. The second field study was conducted in June 2005 to collect the data for elevated releases that were not obtained in the 2004 study. The following sections discuss these two field studies in detail.

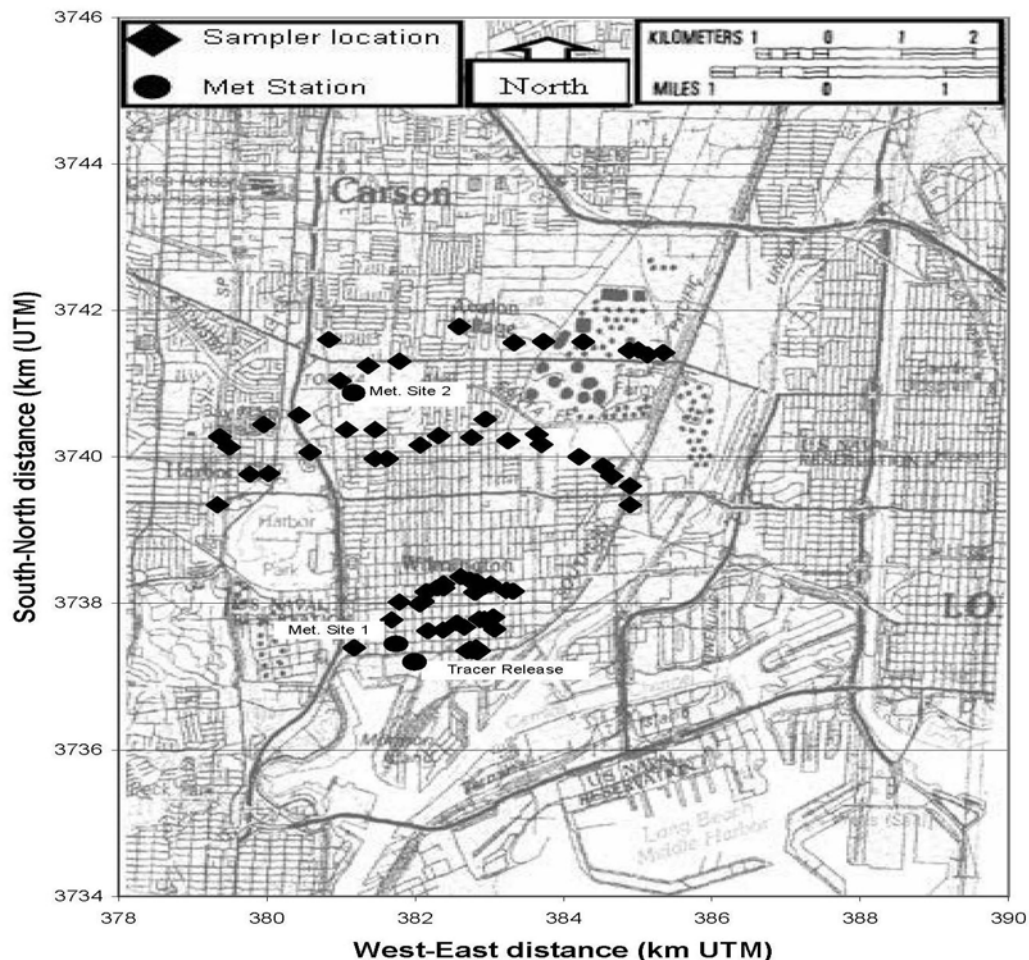
2.2. Wilmington 2004 Study

2.2.1. Concentration and Meteorological Measurements

Tracer Concentration Measurements

Tracer release experiments were conducted on eight days during the period August 26 to September 10, 2004. On each of these days, the tracer gas, sulfur hexafluoride (SF_6) was released from the source over periods lasting from two to six hours. For the first six experiments, pure SF_6 was metered with a mass flow controller and mixed with 1000 liters per minute (L/min) of ambient air provided by a vane pump to change the buoyancy of the gas to nearly that of the surrounding air. The diluted SF_6 was released—inadvertently as explained earlier—at a rate of

4 grams per second (g/sec) (16 kilograms per hour [kg/hr]) at the base of a stack of the LADWP generating station, which is located approximately 0.8 km from the ocean, adjacent to the Port of Los Angeles. During the last two experiments, the diluted SF₆ was directed into a 3 m tall piece of 1-inch polyvinyl chloride (PVC) pipe supported by a tripod in an open area inside the generating station. However, the break in the release line resulted in the emissions escaping near the dilution pump located behind the power plant. The SF₆ tracer gas release rate was 2 g/sec (8 kg/hr) for these tests.



Base map from U.S. Geological Survey

Figure 2.1. Map of study area and equipment locations for Wilmington 2004 study

Thus, all eight days of the field study corresponded to near-surface releases behind the power plant building. However, the results have been separated from the two periods because the two different arrangements in the release system might have had different effects on the leak from the pump.

The released tracer was sampled along five arcs. Three of the arcs were located at approximately 1000 m, 3000 m, and 5000 m from the release point. The fourth and fifth set of samplers was placed along radial distances ranging between 100 and 400 meters from the source. Eighteen samplers were placed at 6° spacing on the 1000 m and 3000 m arcs, while eight

and eleven samplers were placed approximately 5° apart on the 100 m and 400 m arcs, respectively. There were seventeen samplers on the 5000 m arc, with two additional samplers collocated at the two sites for quality control purposes. The locations of these samplers are also shown in the Figure 2.1. Measurements on a mobile monitoring van using a real-time continuous monitor were used to supplement those from the stationary integrated samplers.

Gas samplers, designed and constructed at University of California at Riverside (UCR), were used to collect integrated samples over consecutive one-hour time periods. Each sampler included a timer that controlled six air-sampling pumps. Each pump was connected to a 4-liter polyethylene bag. A rechargeable battery was used to power the pumps and the timer. Air was delivered to the pumps through a common manifold connected to an external probe that extended to a height of 1 m above ground level. The pressure drop inside the system's individual lines and pump valves prevented cross-contamination among the samples. The sampler was designed to take sequential 1-hour samples for a total of 6 hours. This was accomplished by using a single-board computer programmed to control the relay board that switched power in sequence to pumps. All the equipment was housed in a polyethylene tote box.

The SF₆ concentrations of integrated tracer samples were analyzed using a bank of four UCR constructed gas chromatographs (GC), equipped with a 1/8 inch diameter Molecular Sieve 5A° column, electron capture detectors, and a six-port gas sampling valve with a 2 milliliter (ml) sample loop. This analysis system could be loaded with forty samples to determine their SF₆ concentration simultaneously.

More detailed descriptions of the tracer release schedules and sampling methods can be found in Appendix C. The quality assurance audit report for the 2004 field study can be found in Appendix D.

Meteorological Measurements

Measurements of surface winds and winds aloft (up to approximately 600 m) were made using sonic anemometers and remote sensing acoustic sodars. One sonic anemometer, with its sensor placed at a height of 3 m, and a minisodar were collocated at an open area of the release site. The location of the instruments is shown in Figure 2.1 as “Met. site 1.” A second sonic anemometer at 3 m height and a Model 2000 acoustic sodar were placed in an open area at Los Angeles County Sanitation District’s Joint Water Pollution Control Plant (JWPCP), located approximately 4,000 m downwind of the source. A remote-sensing microwave temperature sounder was used to determine the vertical temperature profile from the surface to 600 meters above ground level at this downwind meteorology monitoring site. The location of the instruments is shown in Figure 2.1 as “Met. site 2.”

The three components of velocity and temperature were sampled at 10 Hertz (Hz) using sonic anemometers. These measurements were used to derive one-hour averaged mean winds and temperatures, standard deviations of the turbulent velocity fluctuations, and turbulent momentum and heat fluxes. Winds and turbulence above the urban canopy was measured

using the minisodar that took measurements from 15 m up to 200 m at a resolution of 5 m, and the full sized sodar which provided information up to heights of 600 m above the ground level.

The meteorological measurements provided vertical profiles of wind speed, turbulence, and temperature, which were used to construct the meteorological inputs of the dispersion model described in this chapter.

Details of the meteorological measurements can be found in Appendix C.

2.2.2. Characteristics of Meteorological Variables

The Wilmington experiment yielded approximately one month of mean wind and turbulence data covering a wide variety of meteorological conditions. An example of the behavior of some of the meteorological variables measured during this period is shown in Figure 2.2, which compares the friction velocities and the kinematic heat fluxes measured at two meteorological sites during two of the experimental days. On 9/3/2004, the friction velocities and heat fluxes follow each other in time, while on 9/9/2004, the friction velocity at the downwind site does not start increasing until 11:00 a.m. The research team suggests that this lack of correlation in time is related to the fact that the height of measurement at the downwind site is within the urban canopy, and is thus likely to be affected by channeling effects. In general, the friction velocities at the downwind site are smaller, which supports the hypothesis that the sonic is within the

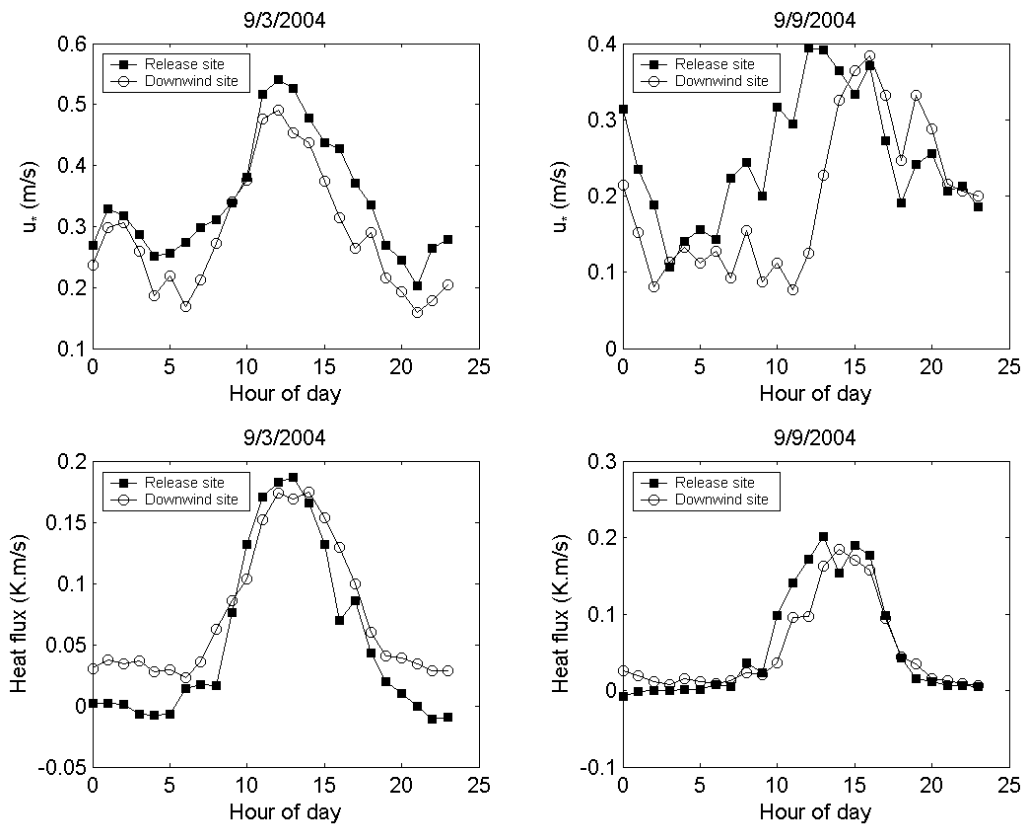


Figure 2.2. Comparison of surface friction velocities and heat fluxes measured by sonic anemometers at LADWP (release site) and JWPCP (downwind site) on 9/3/2004 and 9/9/2004

urban canopy (Rotach 1993). The heat fluxes at the two sites are well correlated in time, with the heat flux in the downwind site being smaller than that at the release site.

The experiments were conducted during daytime hours when the whole area of the field study was dominated by south or southeast onshore flows. The surface boundary layer was convective for most of the experiments, except for the twenty-fourth trial conducted on 9/3/2004 at 7:00 a.m. Figure 2.3 shows profiles of potential temperatures measured on 9/3/2004 at about 4000 m inland from the shore. The boundary layer was still stable before 8:00 a.m. The convective boundary layer started developing around 9:00 a.m., reached a height of 170 m at noon, and did not grow any higher during the course of the day.

The time evolution of these profiles is typical of those observed during the six hours of the day during which the field study was conducted. The profiles show a surface superadiabatic layer capped by a deep stable layer. This structure was observed by Edinger (1963) in his study of the Los Angeles marine layer, which refers to the layer that is in equilibrium with the offshore water surface. This layer, typically 300 m deep, is marked by a homogeneous distribution of water vapor. Subsidence creates the stable potential temperature gradient in the marine layer. The superadiabatic layer, created by surface heating over land, is shallower than the marine layer near the coast; convection eventually burns off the marine layer at some distance inland. Edinger (1963) suggests that thermals originating from the super adiabatic layer are buoyant enough to penetrate the bulk of the moist stable layer capping it. The thermals become negatively buoyant only when they encounter the dry warm air above the marine layer. This picture of the thermal internal boundary layer that forms near the Los Angeles coastline is considerably more complicated than that used to formulate models for the growth of the TIBL: an adiabatic layer separated from a capping stable layer by a sharp temperature jump. It suggests that the vertical mixing can extend beyond the height of the surface based superadiabatic layer. These observations are consistent with those of Gamo et al. (1982) in their study of sea-breeze events in the east coast of Japan, where they report that the TIBL top—defined from the potential temperature profile—is well below the level of minimum turbulent kinetic energy. Indirect evidence from the analysis of concentrations described in Section 2.2.4, supports this suggestion.

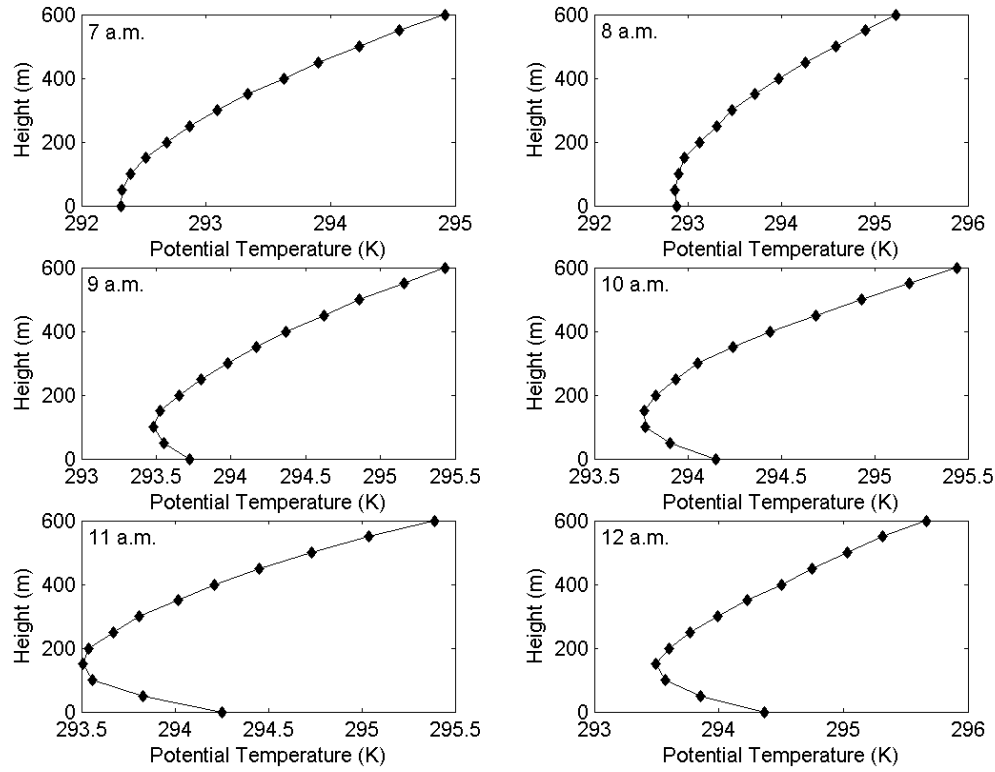


Figure 2.3. Profiles of potential temperatures measured on 9/3/2004 at downwind site

Figure 2.4 shows an example of the meteorological profiles for hour 7 on September 3, measured by the minisodar at the release site. The coordinate system used here has its x-axis along the east-west direction, and y-axis along the north-south axis. The u component refers to the x-axis, and the v component to the y-axis. The mean velocity shown in the figure is the magnitude of the mean vector wind. The lateral turbulent velocity σ_v corresponds to a coordinate system in which the x-axis lies along the mean wind, and is obtained from the horizontal turbulent velocity fluctuations measured in the east-west and north-south coordinate system.

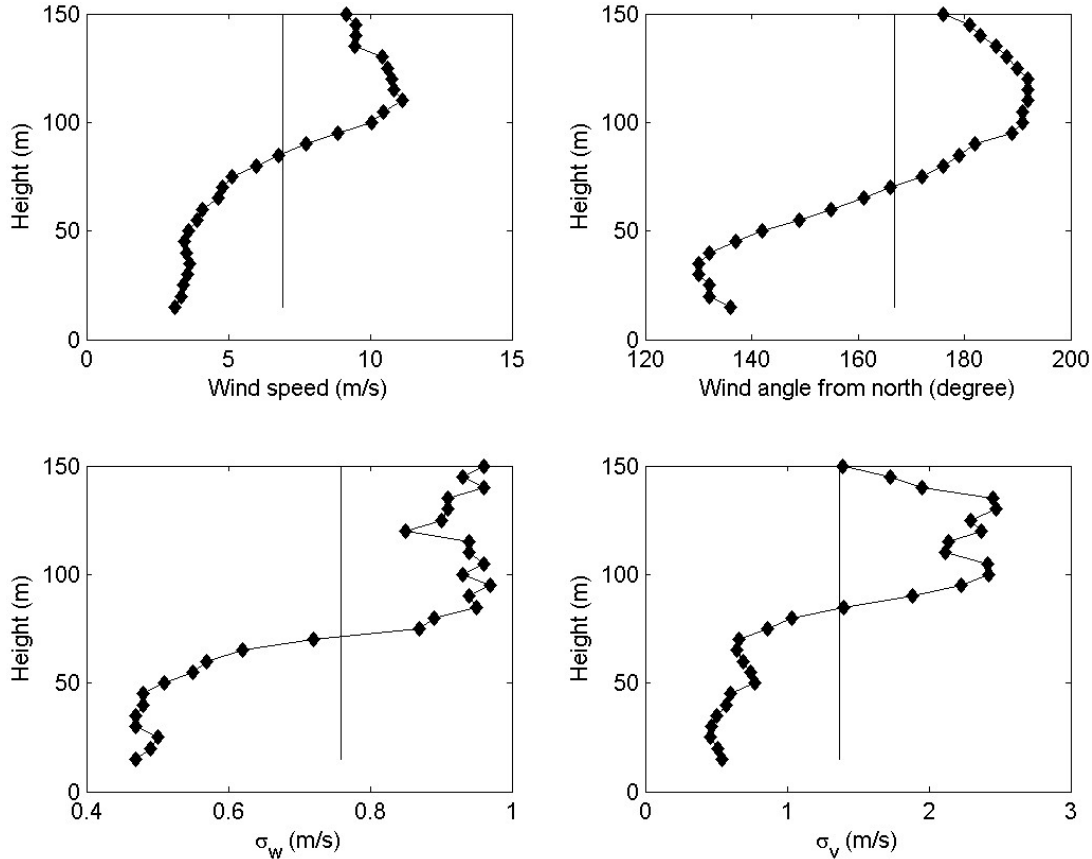


Figure 2.4. Meteorological profiles observed on hour 7 on 9/3/2004 at the release site. Vertical lines represent mean values of the variables.

Figure 2.4 indicates that the turbulence extends through 150 m, even though the temperature profiles of Figure 2.3 indicate that boundary layer is stable above 100 m at 7:00 a.m. However, because the noise-to-signal ratio approaches unity above 50 m, the rapid increase in σ_w and σ_v above 70 m might not be real.

In an earlier analysis of the data (Yuan et al. 2006), the research team hypothesized that the vertical extent of turbulent mixing is determined by the height of a shear generated boundary layer that is advected with the onshore flow. This hypothesis was supported by the observed behavior of ground-level concentrations. However, the analysis of the tracer data corresponding to the elevated releases in 2005 indicated the presence of a convective internal boundary layer that forms when cold air from the ocean flows onto warmer land (Venkatram 1977). Thus, the research team reanalyzed the data collected in August 2004 using the model developed to explain the data from the tracer experiment conducted in June 2005. The next section presents the results of this analysis.

2.2.3. Dispersion Parameters

The solar data were considered reliable over the height range extending from 15 m to about 50 m. Because the turbulence levels did not vary significantly over this height range, the research team took the measured values at 50 m to be representative of the boundary layer (BL). These values were used as inputs to the dispersion model, which is described next.

Figure 2.5 shows the range of meteorological variables sampled in the field experiment. The turbulent intensities vary from 0.17 to as large as 1.1 during an hour in which the wind speed dropped below 1 m/s. The mean horizontal intensity is 0.21 while the mean vertical intensity is 0.19. The transport winds used in the model vary from less than 1 m/s to 5 m/s.

A summary of the meteorological measurements is provided in Appendix E.

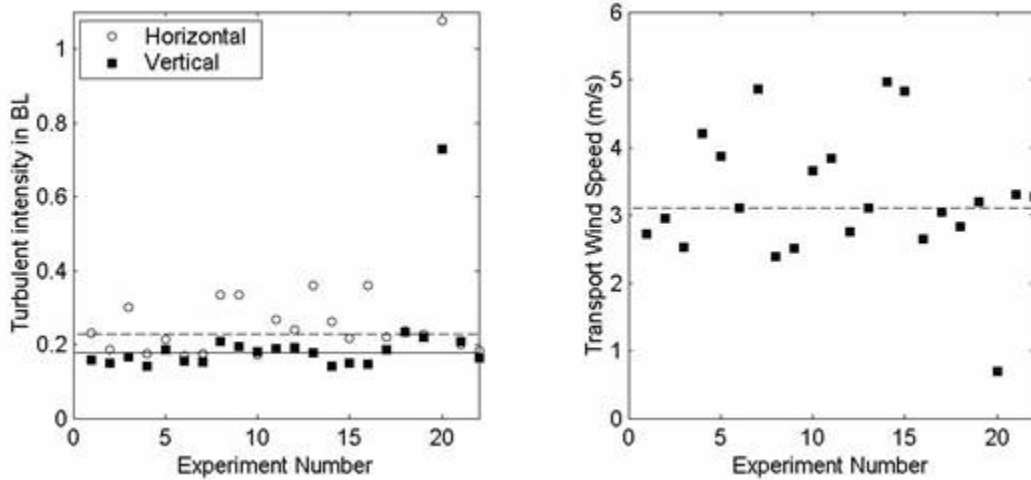


Figure 2.5. Variation of turbulent intensities and transport wind speeds used in the dispersion model for Wilmington 2004 study. Horizontal lines correspond to mean values of the variables.

The research team estimated the horizontal plume spreads by assuming that the maximum concentration measured on each arc corresponded to the plume centerline. Researchers assumed that σ_y did not vary along the arc so that the concentrations were described by:

$$C(x, y) = C_{\max} \exp\left(-\frac{y^2}{2\sigma_y^2}\right). \quad (2.1)$$

Then, σ_y was obtained by fitting the following equation to the data from each arc:

$$\ln\left(\frac{C_{\max}}{C}\right) = \frac{1}{2\sigma_y^2} y^2. \quad (2.2)$$

where C_{\max} is the maximum concentration (ppt), C is the concentration (ppt), y is the crosswind distance (m), and σ_y = crosswind horizontal plume spread (m).

The slope of the fitted line was used to compute σ_y . The research team adjusted the σ_y determined from Equation (2.2) until the team obtained the best fit between estimated and observed concentrations along each arc. Figure 2.6 shows examples of estimated concentration profiles compared with observed concentrations on hour 11 on September 2, 2004.

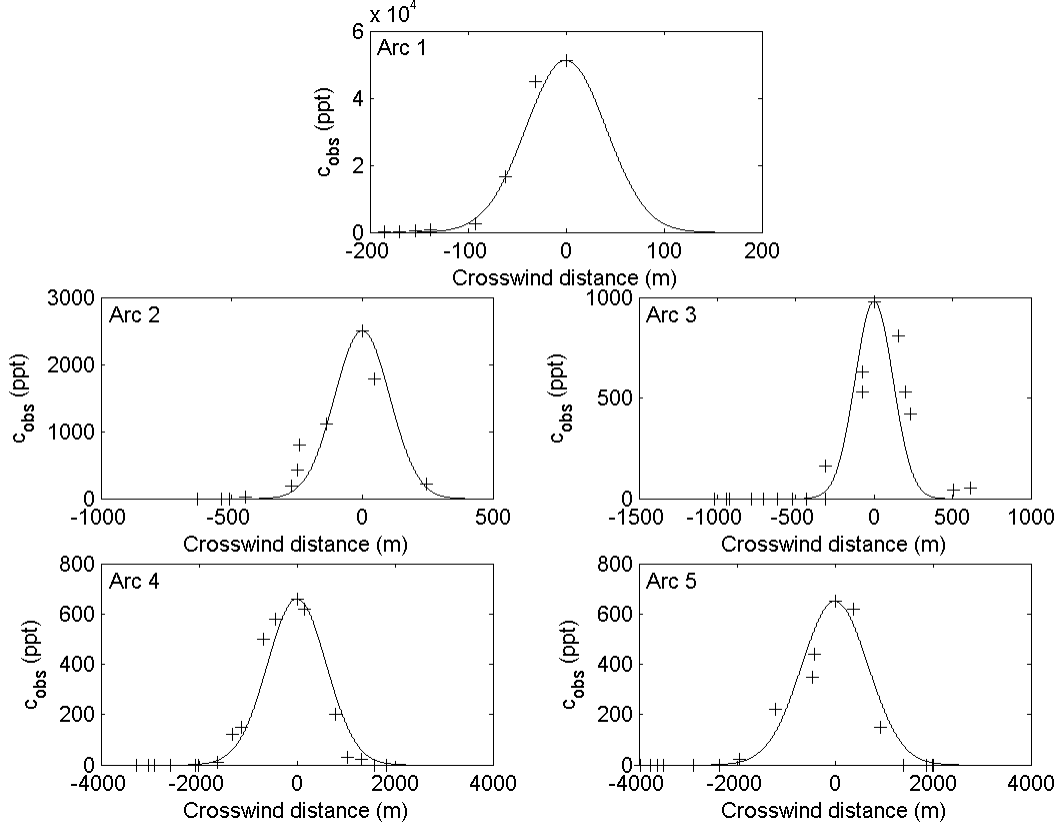


Figure 2.6. Crosswind concentration profiles measured from ground-level releases on 9/2/2004 at 11:00 a.m. Arcs 1 through 5 are 100 m, 400 m, 1000 m, 3000 m, and 5000 m from source, respectively.

The vertical plume spreads were inferred from a Gaussian dispersion model using the arc maximum ground-level concentration and the mean wind discussed earlier:

$$\sigma_z = \frac{Q}{\pi U \sigma_y C_{\max}}, \quad (2.3)$$

where Q is the source strength, and U is the transport wind speed at 50 m, and σ_z is the vertical plume spread (m) .

Figure 2.7 shows the variations of the observed horizontal and vertical plume spreads with downwind distances over all the runs for two sets of experiments: one corresponding to releases inside the cluster of buildings in the LADWP power plant, and the other to releases in an open area close to the power plant. The first set of releases was conducted during the first six days of the experiment, and the second set during the last two days. As indicated earlier,

both sets of releases occurred near the ground, with most of the tracer escaping near the pump of the release system.

The dashed straight lines in the figures correspond to the equations $\sigma_z = i_z x$ and $\sigma_y = i_y x$, where x is the distance from the source (m) and where $i_z = \sigma_w/U$ and $i_y = \sigma_v/U$ are the vertical and horizontal turbulent intensities. Figure 2.7 shows that σ_z first grows rapidly and then levels off around 1000 m from the release. The non-monotonic changes in σ_z with distance seen in the figures are caused by the assumption in Equation (2.1) that the observed arc maximum corresponds to the centerline concentration. It is likely that the samplers at the arcs less than 1000 m from the source missed the centerline concentration of the plume, which means that using the observed arc maximum in Equation (2.3) would overestimate the vertical plume spread. The figure shows that the growth of σ_z is limited by the height of the internal boundary layer, which is discussed in detail in the next section.

The growth rate of the observed horizontal spread is less than linear and can be represented by the equation:

$$\sigma_y = \frac{i_y x}{(1 + x/L_y)^{1/2}}, \quad (2.4)$$

where i_y is the horizontal turbulent intensity at a height of 50 m. The length scale, L_y , was taken to be 2500 m, a value suggested by Briggs (1973) for use in urban areas on the basis of his analysis of the St. Louis experiment (McElroy and Pooler 1968).

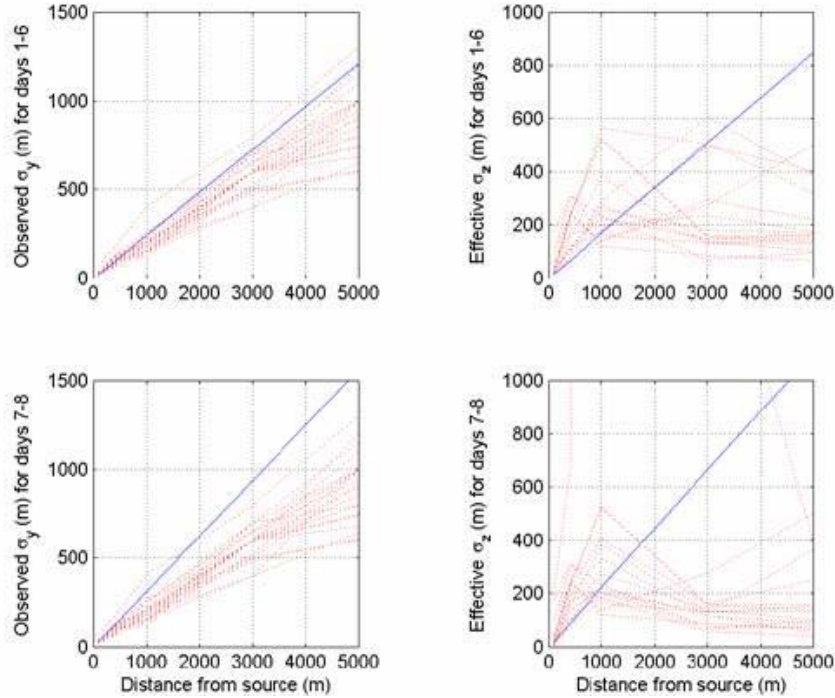


Figure 2.7. The variation of dispersion parameters as a function of downwind distance for the Wilmington 2004 study. The solid straight lines represent linear growth determined by the mean turbulent intensities.

Figure 2.8 indicates that estimates of σ_y from Equation (2.4) compare well with observed values for the first six days (Figure 2.8a) as well as the last two days (Figure 2.8b) of experiments. It appears that there is no need to invoke building-induced horizontal plume spread to explain the observations of horizontal plume spread.

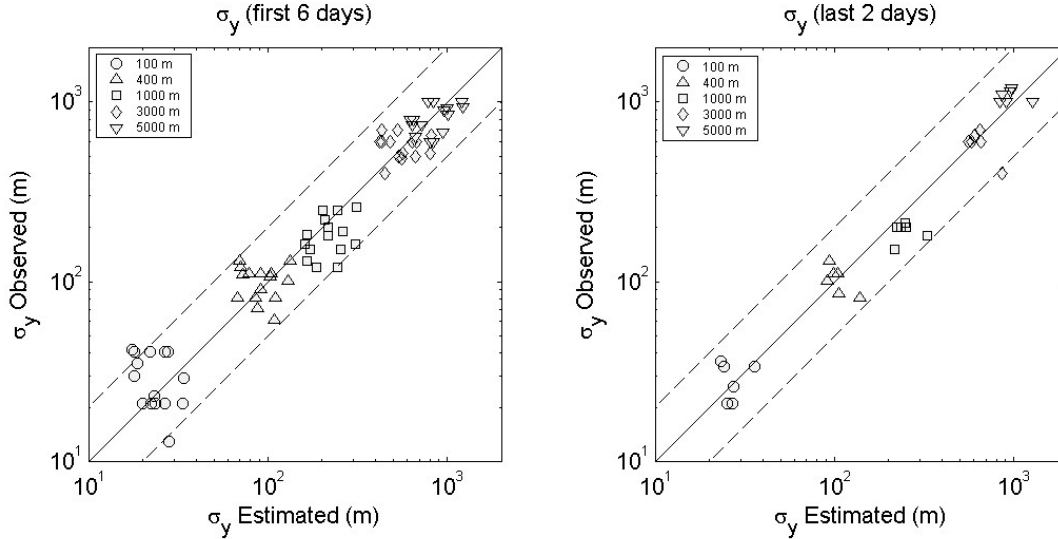


Figure 2.8. Comparison of measured horizontal plume spreads with model estimates during the (a) first six days and (b) last two days of the Wilmington 2004 study

2.2.4. Analysis of Concentrations

Figure 2.9 shows the variation of the arc maximum concentrations with distance from release; each point is obtained by averaging over maximum concentrations observed at each arc. The straight lines correspond to $C_{\max} \sim 1/x^2$, which is the variation that would result if the plume spreads grew linearly with distance. The concentrations decrease at a slower rate than x^2 after a distance of about 1000 m from the source. There is little difference in the variation of concentrations for the two sets of releases except close to the source. The research team does not have a good explanation for the higher near source concentrations during the last two days of the field study. More details of the tracer sampling are presented in Appendix F.

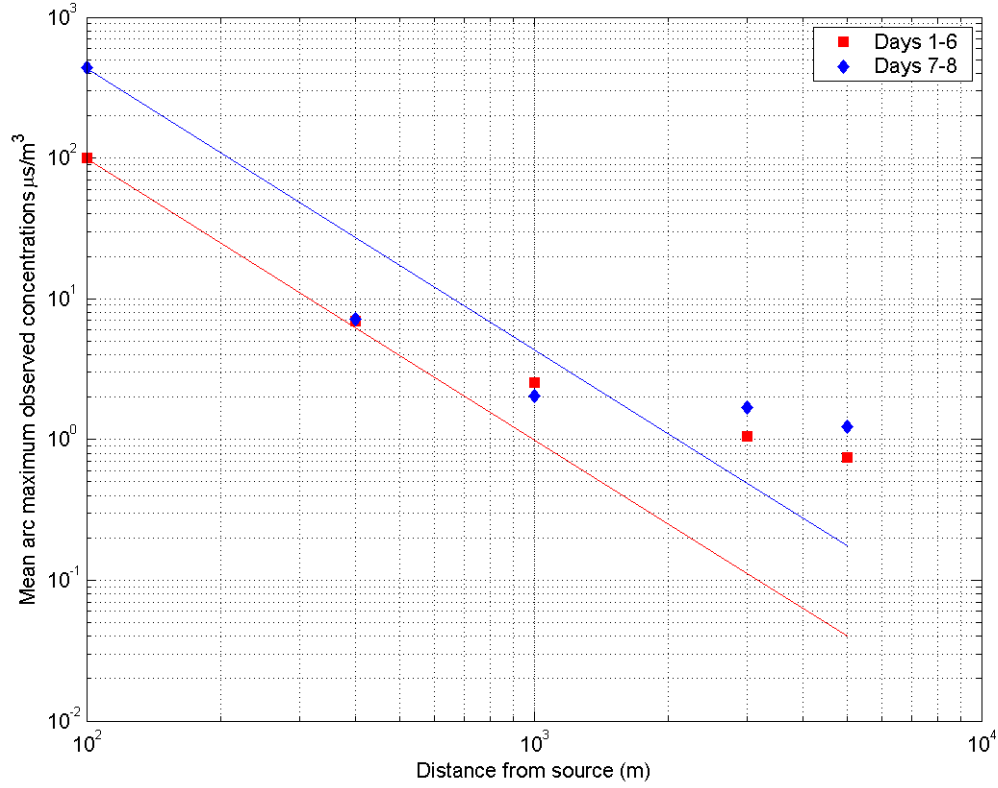


Figure 2.9. The variation of observed arc maximum concentrations from ground-level releases with downwind distance for the Wilmington 2004 study

These measured maximum concentrations were analyzed using a dispersion model that assumes Gaussian distributions in the horizontal and vertical directions. The concentration is given by:

$$\frac{C(x, y=0, z=0)}{Q} = \frac{1}{\pi U \sigma_y \sigma_z} \exp\left(-\frac{h_s^2}{2\sigma_z^2}\right), \quad (2.5)$$

where $C(x, y=0, z=0)$ is the downwind ground level concentration in micrograms per cubic meter ($\mu\text{g}/\text{m}^3$), Q is the source strength in micrograms per second ($\mu\text{g}/\text{s}$), x is the downwind distance from release (m), h_s is the release height (m), and U is the transport wind speed (m/s), σ_y is the horizontal plume spread (m), and σ_z is the vertical plume spread (m). The horizontal plume spread is given by Equation (2.4). The vertical spread is taken to be:

$$\sigma_z = \frac{\sigma_w x}{U}. \quad (2.6)$$

Model performance is described in terms of the statistics of the ratio C_p/C_o , where C_o and C_p refer to the observed and predicted concentrations, respectively. Then, the bias in the model estimate is given by m_g , the geometric mean of the ratio:

$$m_g = \exp(\text{mean}(\varepsilon))$$

where

(2.7)

$$\varepsilon = \log\left(\frac{C_p}{C_o}\right)$$

and the spread of observations about a model estimate is quantified using the geometric standard deviation, s_g ,

$$s_g = \exp(\text{standard deviation of } \varepsilon).$$
(2.8)

Then if the observed concentrations are lognormally distributed about the model estimate the 95% confidence of the ratio of the observed to the estimated concentration is given by the interval $m_g s_g^{1.96}$ to $m_g s_g^{-1.96}$. When appropriate, one may also use r^2 , the coefficient of determination between the logarithms of C_o and C_p , to measure model performance.

In this study's first analysis of the 2004 data, presented in Yuan et al. (2006), the research team suggested that mixing in the vertical was limited by the height of a shear-generated boundary layer h_{sh} , given by

$$h_{sh} = 8 \frac{\sigma_w}{N},$$
(2.9)

where N is the Brunt-Vaisala frequency (s^{-1}),

$$N = \left(\frac{g}{T_o} \gamma \right)^{1/2},$$
(2.10)

where γ is the gradient of the potential temperature profile above the convective internal boundary layer (K/m), and T_o is the surface temperature (K), and g is the acceleration due to gravity (9.81 m/s^2).

The research team suggested that shear rather than buoyancy controlled the height of the boundary layer because the measured temperature profiles (See Figure 2.3) implied convective boundary layers that were about a factor of two smaller than those inferred from the ground-level concentrations. However, an analysis of the tracer data from the experiment conducted in June 2005 suggested that the ground-level concentrations from the elevated buoyant release could be explained only by incorporating a thermal internal boundary layer that grew with distance from the shoreline. This realization forced the research team to reexamine the data from August 2004. Specifically, researchers wanted to discover whether modeling the boundary layer as a growing convective internal boundary layer could explain the data that were analyzed earlier using a shear-generated boundary layer to limit vertical mixing.

As the first step in the reanalysis, this report shows that Equation (2.9) is consistent with the equation describing the development of the convective internal boundary layer. A model (Venkatram 1977) for internal boundary growth predicts the height z_i

$$z_i = \left(\frac{2Q_o(1+2A)x}{U\gamma} \right)^{1/2},$$
(2.11)

where Q_o is the average kinematic heat flux over land (K·m/s), A is the ratio of the inversion to the surface heat flux, x is the distance from the shoreline (m), and U is the boundary layer-averaged wind speed (m/s).

If one assumes that the measured vertical velocity fluctuations are dominated by convection, then

$$\sigma_w = \alpha \left(\frac{g}{T_o} Q_o z_i \right)^{1/3}, \quad (2.12)$$

where $\alpha = 0.6$ (Stull 1988). Substituting Equation (2.11) into Equation (2.12), and using the definition of the Brunt-Vaisala frequency in Equation (2.10) it is found that

$$z_i = \frac{\sigma_w}{N} \left(\frac{Nx}{U} \right)^{1/3} \frac{(2(1+2A))^{1/3}}{\alpha}. \quad (2.13)$$

Using values of $N = 0.017 \text{ s}^{-1}$, $U = 3 \text{ m/s}$, $x = 5000 \text{ m}$, and $A = 0.25$ (Venkatram 1977), which are typical of the Wilmington experiment, the term multiplying σ_w / N is about 7.3 m, which is consistent with the empirically determined value of 8 m. The meteorological variables within the parenthesis on the right hand side of the equation do vary with experiment, but z_i depends only on the 1/3 power of N/U .

In view of the earlier discussion on the structure of the TIBL, Equation (2.11) might not provide realistic estimates of the height of the TIBL. But in the absence of an alternative, the research team retains the form of the equation but introduces empirical parameters as follows:

$$z_i = a \left(\frac{2Q_o(x + x_o)}{U\gamma} \right)^{1/2}. \quad (2.14)$$

The parameter x_o is the distance of the effective shoreline from the release, which cannot be objectively determined in view of the complicated geometry of the coastline. Taking $x_o = 100 \text{ m}$ yielded the best agreement between modeled concentrations and observations corresponding to elevated releases. The parameter is empirically determined to be two.

Figure 2.10 shows the variation of the TIBL height at 5000 m from the shoreline, calculated with Equation (2.14). The figure shows 22 values from all eight days of the field study when the wind was southerly and concentrations were detected at the samplers. The dotted line does not signify a time sequence, although points showing increases of the TIBL height correspond to successive hours of the experiment on each day of the experiment. The TIBL height varies from 200 m at the beginning of each day of study, typically 7:00 a.m., to about 600 m around 12:00 p.m., when the tracer release ended.

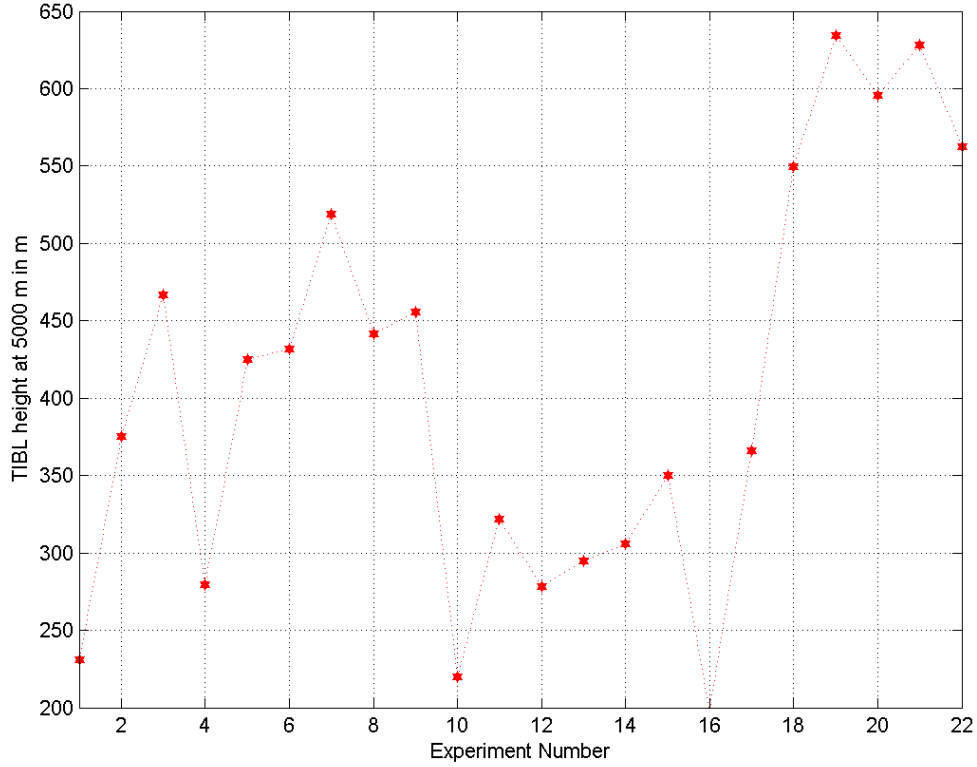


Figure 2.10. Variation of the TIBL height at 5000 m during Wilmington 2004 study

The left panels of Figure 2.11 compare observed ground-level concentration maxima, normalized by the emission rate, with estimates using Equations (2.4) and (2.6) for plume spread. The plots, which compare the estimated maximum on each arc with the observed maximum on the same arc, show that the model overestimates the concentrations in the first two arcs but underestimates the ground-level concentrations on the 3000 m and 5000 m arcs.

The right panels of Figure 2.11 show the effects of making two modifications to the model. The first involves using an initial vertical plume spread, σ_{zo} , induced by the power plant building behind which the releases occurred. If it is assumed that the plume is well mixed through the building height of 40 m, σ_{zo} works out to be 32 m, which is $\sqrt{2/\pi} = 0.8$ times the height of the building. Incorporating initial plume spread eliminates the overestimation on the 100 m arc.

The second modification is associated with limiting vertical dispersion to the height of a boundary layer, given by Equation (2.14). The vertical plume spread is modified to

$$\sigma_z = \min\left(\frac{\sigma_w x}{U}, \sqrt{\frac{2}{\pi}} z_i\right). \quad (2.15)$$

This reduces the underestimation of concentrations on the 3000 m and 5000 m arcs, as seen in the right panels of Figure 2.11. These changes in the model decrease the geometric standard deviation, s_g for both sets of releases. But the model still overestimates the maximum arc concentrations at 100 and 400 m, which might indicate that the observed concentrations do not correspond to the centerline concentrations estimated by the model.

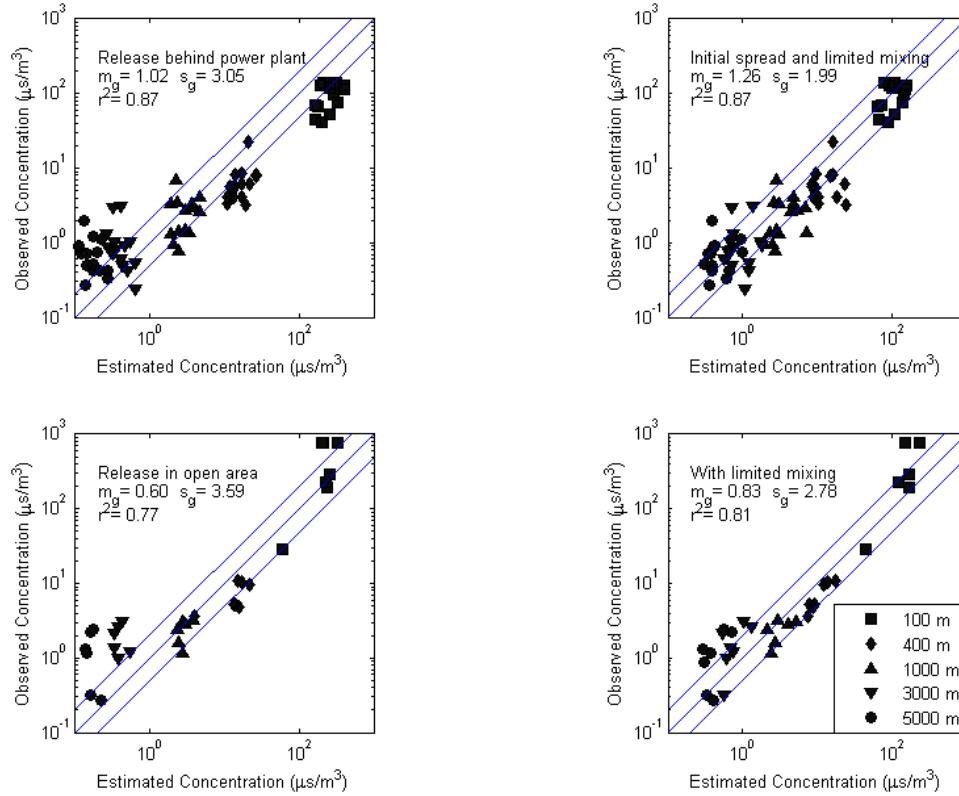


Figure 2.11. Comparison of measured arc maximum concentrations from ground-level releases with model estimates during the first six days (upper panels) and the last two days (lower panels) of Wilmington 2004 study. Right panels correspond to modifications described in the text.

The next section describes the 2005 experiment, which was designed to examine dispersion from elevated sources.

2.3. Wilmington 2005 Study

2.3.1. Experimental Design and Implementation

The 2005 field study was conducted near LADWP between June 24 and June 28 2005. The objective of this field study was to collect tracer data that would allow the development and testing of a dispersion model applicable to elevated releases in coastal urban areas.

Each experiment involved release of the tracer gas, SF_6 , over periods lasting from 5 to 6 hours during each day of the four-day experiment. Two sets of experiments were conducted. During the studies conducted on June 24 and June 27, SF_6 was metered at 4 g/sec (16 kg/hr) and was introduced into the base of the 67 m high stack to allow it to become well mixed with the stack exhaust. The inner diameter of the stack is 4.7 m, and the exit velocity and temperature of the exhaust gases are 23 m/s and 458 K, respectively. The plume buoyancy parameter works out to be $431 \text{ m}^4/\text{s}^3$, which results in a plume rise of about 175 m for the meteorological conditions observed during the field study.

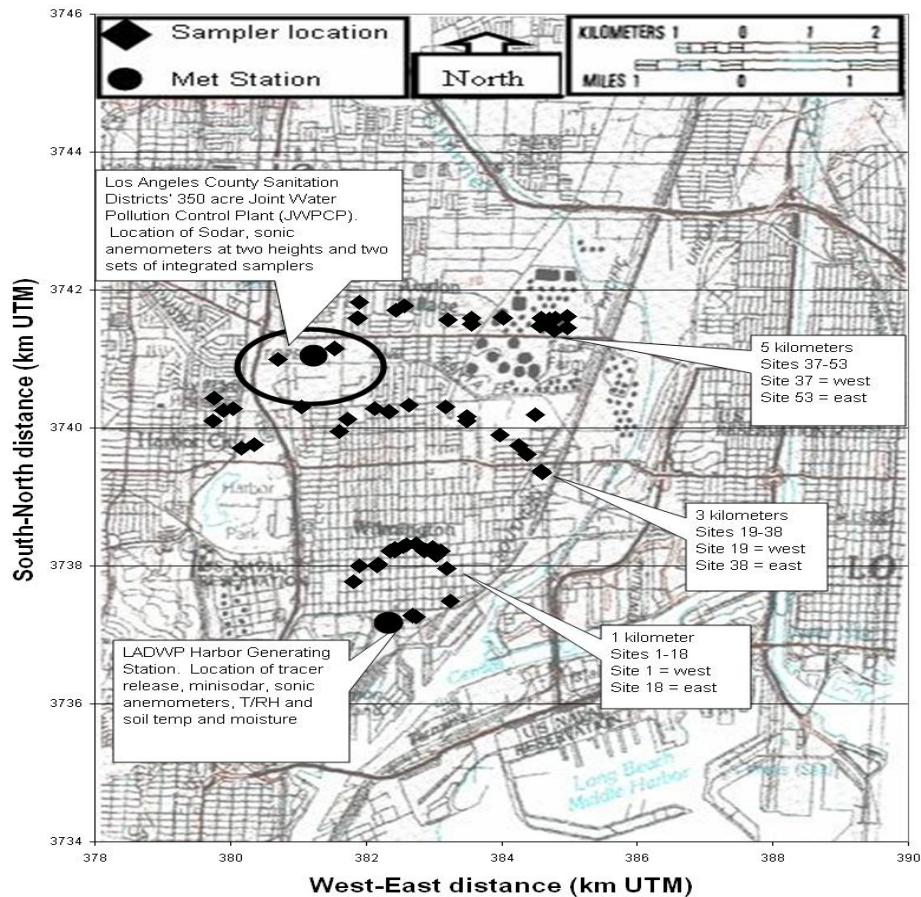
During the remaining two days, June 26 and June 28, pure SF₆ was metered with a mass flow controller and mixed with 1000 L/min of ambient air provided by a vane pump to change the buoyancy of the gas to nearly that of the surrounding air. The diluted SF₆ was released at a rate of 4 g/sec (16 kg/hr) outside the stack and about 3 m below the stack top. Figure 2.12 shows the layout of the study area and the locations of the tracer release and sampling equipments. These two different tracer releases were designed to understand the effect of release height on ground-level concentrations.

Researchers placed a minisodar, two sonic anemometers (with their sensors at heights of 3 and 6 m), soil moisture and surface temperature sensors, and temperature and relative humidity measurement systems near the western fence line of the power plant, approximately 100 m away from the plant stacks.

A second minisodar was located approximately 4 km further inland on the JWPCP. A three-axis sonic anemometer with its sensors at heights of 7 m was also located at this facility. The temperature from near surface to up to about 600 meters was measured at this facility using a remote sensing microwave temperature profiler.

Integrated box samplers were deployed along three arcs with distances of 1000 m, 3000 m, and 5000 m north to the source. The samplers were placed about 6° apart. Because the research team anticipated that the wind direction would vary over about 90° during the course of the planned sampling period, it was necessary to place a minimum of 16 samplers at each sampling arc, to ensure sampling of the plume.

More details on meteorological measurement, tracer release, and sampling are provided in Appendix G. The quality assurance audit report for the 2005 study can be found in Appendix H.



Base map from U.S. Geological Survey

Figure 2.12. Map of study area and equipment locations for the Wilmington 2005 study

2.3.2. Modeling

Model Formulation

Figure 2.13 compares the concentrations observed during the two sets of experiments: one corresponding to the release 3 m below stack height, and the other corresponding to the release into the exhaust gases. The left panel shows that concentrations resulting from the in-stack buoyant release results in concentrations around 0.1 microsecond per cubic meter ($\mu\text{s}/\text{m}^3$) at a distance of 1 km, which then increase to about 0.5 $\mu\text{s}/\text{m}^3$ at distances between 3 and 5 km. The concentrations for the below stack top release at 64 m behave similarly to the surface releases conducted in 2004: the concentrations decrease with distance. Most of the observations are above 1 $\mu\text{s}/\text{m}^3$ at 1 km from release, and decrease to about 0.4 $\mu\text{s}/\text{m}^3$ at 5 km. Note that at 3 and 5 km, the observed concentrations for the in-stack and below stack releases are similar in magnitude.

The relatively slow increase in concentration with distance for the in-stack release suggests the entrainment of an elevated plume by a growing internal boundary layer (Misra 1980). This

observation suggested that the earlier hypothesis (Yuan et al. 2006) about the shear-generated boundary layer was incorrect.

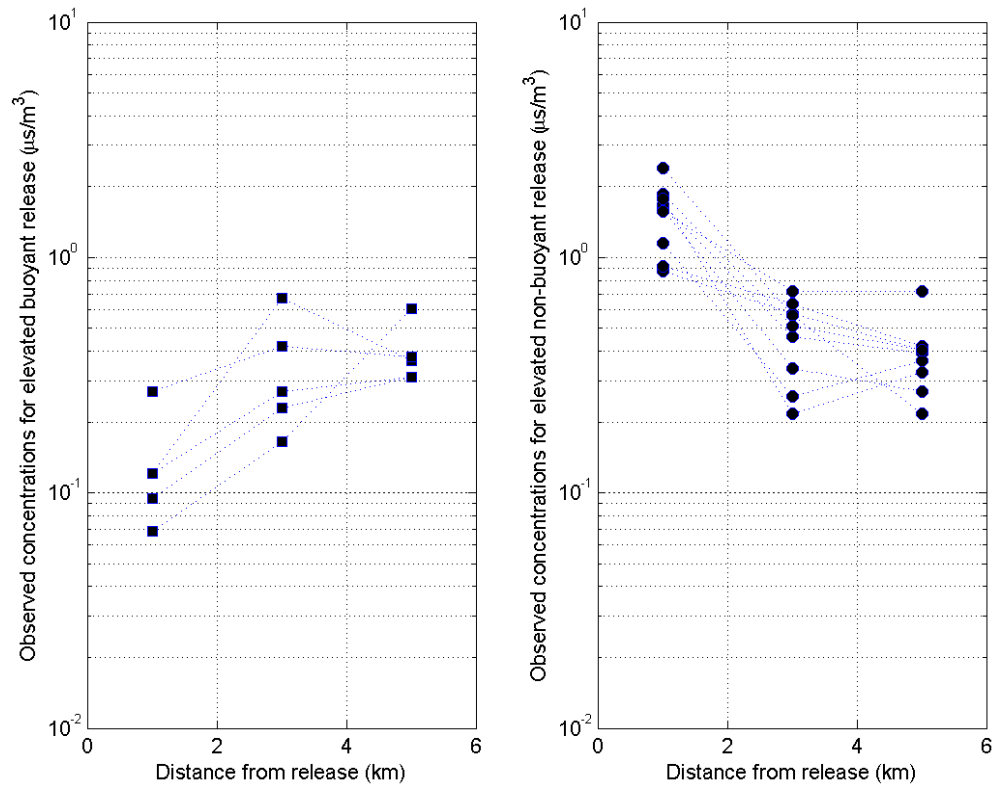


Figure 2.13. The variation of observed arc maximum concentrations with downwind distance for elevated releases into stack and below stack top for the Wilmington 2005 study

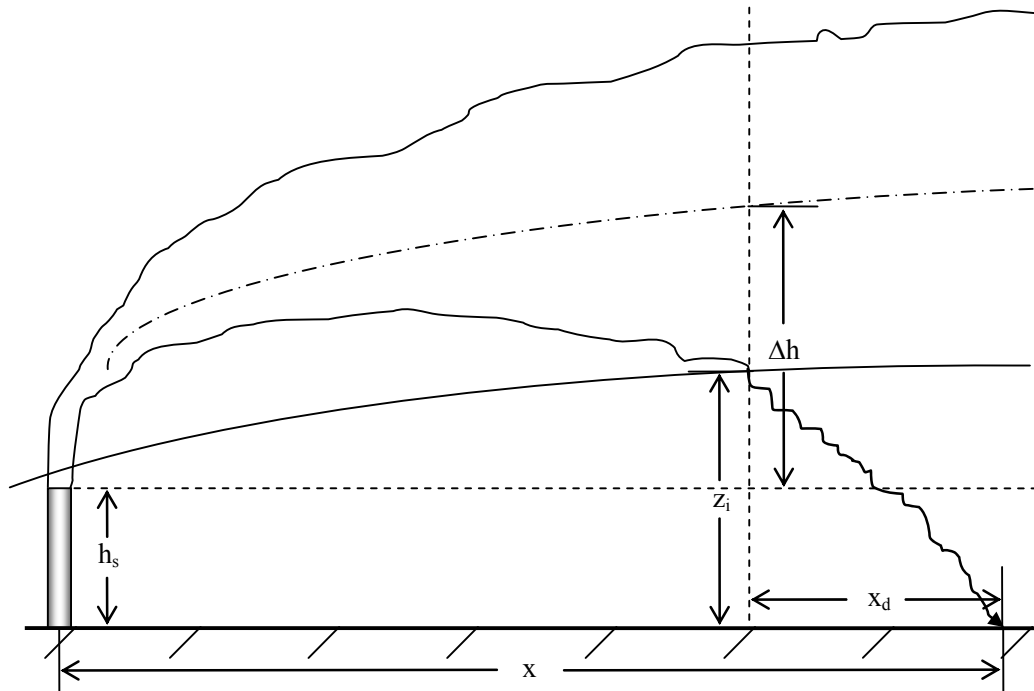


Figure 2.14. Entrainment of plume by growing internal boundary layer

The dispersion model used to interpret the data was similar to that developed by Van Dop et al. (1979) and improved by Misra (1980). The model was evaluated by Misra and Onlock (1982) with data collected in a dispersion experiment conducted in the vicinity of the Nanticoke power plant on the north shore of Lake Erie. The research team modified the model to incorporate the measurements of turbulence made in the Wilmington experiment.

Misra's (1980) model is based on the following physical picture. As the elevated plume is transported above the internal boundary layer, it grows both horizontally and vertically due to atmospheric turbulence and turbulence generated by plume buoyancy. Because atmospheric turbulence is small above the TIBL, plume buoyancy generates most of the plume growth. This growing plume is entrained by the TIBL, whose height increases with distance from the shoreline (Figure 2.14). The entrained plume material is rapidly mixed to ground-level by the vigorous convective motions within the internal boundary layer.

The gradual entrainment of the elevated plume by the internal boundary layer is modeled by Misra (1980) as a series of point sources whose strength depends on the rate of entrainment by the TIBL and the vertical growth of the plume. Assuming that the entrained plume material is instantaneously mixed through the depth of the TIBL, the ground-level concentration is given by the sum of the contributions of all the upwind point sources. The expression for the centerline ground-level concentration is given by Misra (1980):

$$C(x,0,0) = \frac{Q}{\sqrt{2\pi}Uz_i} \int_{-\infty}^p \frac{1}{\sigma_{yc}} \exp(-t^2) dt, \quad (2.16)$$

where Q is the release rate; and z_i is the height of the TIBL at the distance x . The variable t (s) is related to x' (m), the location of the point source, through

$$t = \frac{(z_i(x') - h_e)}{\sqrt{2}\sigma_{zs}(x')}, \quad (2.17)$$

where h_e is the effective stack height (m), and σ_{zs} is the vertical plume spread above the internal boundary layer (m). The upper limit of the integral is $p = t(x' = x)$.

The horizontal plume spread in Equation (2.16) is given by

$$\sigma_{yc}^2 = \sigma_{ys}^2(x') + \sigma_{yu}^2(x - x'). \quad (2.18)$$

In Equation (2.18), σ_{ys} is the horizontal spread in the layer above the internal boundary layer (m), and σ_{yu} is the horizontal within the TIBL (m). Note that the effective horizontal plume spread combines two spreads; the plume spread in the layer above the TIBL over the distance 0 to x' , and then in the TIBL over the distance $(x - x')$.

Sensitivity studies with the model suggested that best results were obtained when σ_v above the TIBL was taken to be same value as that within the TIBL. This allows us to combine the two terms in Equation (2.18) to obtain an expression for the horizontal plume spread as a combination of that caused by turbulence and that due to plume buoyancy:

$$\sigma_{ye} = \sqrt{\sigma_y^2 + \sigma_s^2}, \quad (2.19)$$

Where σ_y is given by Equation (2.4) derived from the 2004 experiments, and σ_s is the plume buoyancy induced spread (m), which is discussed later. It turns out that Equation (2.4) is consistent with the horizontal spreads derived from data collected in the 2005 experiments.

The vertical spread, σ_{zs} (m), is taken to be

$$\sigma_{zs} = \sqrt{\left(\frac{\sigma_{ws}x}{U}\right)^2 + \sigma_s^2}, \quad (2.20)$$

where the vertical turbulence, σ_{ws} (m/s) is taken to be a nominal value of 0.001 times the value in the internal boundary layer.

Because the horizontal plume spread is not a function of t , as assumed in Equation (2.4), it can be taken outside the integral in Equation (2.16) to obtain

$$C(x,0,0) = \frac{\text{frac}}{\sqrt{2\pi}U\sigma_{ye}z_i}, \quad (2.21)$$

where frac, the fraction of the plume entrained into the TIBL, is

$$\text{frac} = \frac{1}{2} \left(1 - \text{erf} \left(\frac{z_i - h_e}{\sqrt{2}\sigma_{zs}} \right) \right), \quad (2.22)$$

where erf is the error function.

In Equation (2.22), the effective stack height (m) is

$$h_e = h_s + \Delta h, \quad (2.23)$$

where h_s (m) is the physical stack and plume rise (m) is given by:

$$\Delta h = \min \left(1.6 \frac{F_b^{1/3}}{U} x^{2/3}, 2.6 \left(\frac{F_b}{U_s} \right)^{1/3} \right), \quad (2.24)$$

where the buoyancy parameter F_b (m^4/s^3) is defined as

$$F_b = gV_s \left(\frac{D_s}{2} \right)^2 \frac{T_s - T}{T_s}, \quad (2.25)$$

where V_s , T_s , and D_s are the exhaust velocity (m/s), temperature (K), and diameter of the stack (m); T (K) is the ambient temperature.

The stability parameter s ($1/\text{s}^2$) is defined as

$$s = \frac{g}{T_o} \frac{d\theta}{dz}. \quad (2.26)$$

Self-induced plume spread (m) is related to plume rise (m) through

$$\sigma_s = \frac{\beta \Delta h}{\sqrt{2}}, \quad (2.27)$$

where the entrainment coefficient $\beta = 0.6$.

The concentration at x is determined by the material entrained at upwind distances $x' < x$. But only a fraction of the material that is entrained into the TIBL is well mixed through the boundary layer depth at the distance x . This needs to be accounted for in Equation (2.21), which assumes that the material is well mixed through z_i . To do so, one must first calculate the distance x_d (m) required for a release to become well mixed by the time it reaches x (Figure 2.14). This distance is given by,

$$\sqrt{\frac{2}{\pi}} z_i = \frac{\sigma_w x_d}{U}, \quad (2.28)$$

where z_i (m) is the boundary layer height at x . Then, frac in Equation (2.22) is evaluated at the reduced distance $(x - x_d)$. Without this modification, the model proposed by Misra (1980) overestimates the concentrations for the elevated release.

The next section describes results from the application of the model to describe the concentration observations described earlier. Note that the model applies to both in-stack and below-stack releases. The buoyancy parameter, F_b , is set to zero and $h_s = 64$ m for the below stack release. The key to the electronic modeling data files can be found in Appendix I.

Model Evaluation

Figure 2.15 shows the variation of the inputs used to model the elevated buoyant release, which occurred between the hours 7 to 11 on June 27, 2005. Data from June 24, the first day of release from inside the stack, are not presented here because the winds were variable, resulting in small concentrations at the samplers. It was not possible to assign a wind direction under these conditions.

The figure shows that the wind speed at 50 m increases from 2.5 m/s to just over 3 m/s during the first hour, and then decreases steadily to 1.5 m/s by hour 11. The maximum TIBL refers to that calculated with Equation (2.14) at distance of 5 km from the source. This height increases from about 200 m at hour 7 to over 700 m at hour 11 in response to the increases in the surface heat flux. As indicated earlier, these heights are generally larger than those inferred from the potential temperature profile measured at the JWPCP site, marked in Figure 2.12.

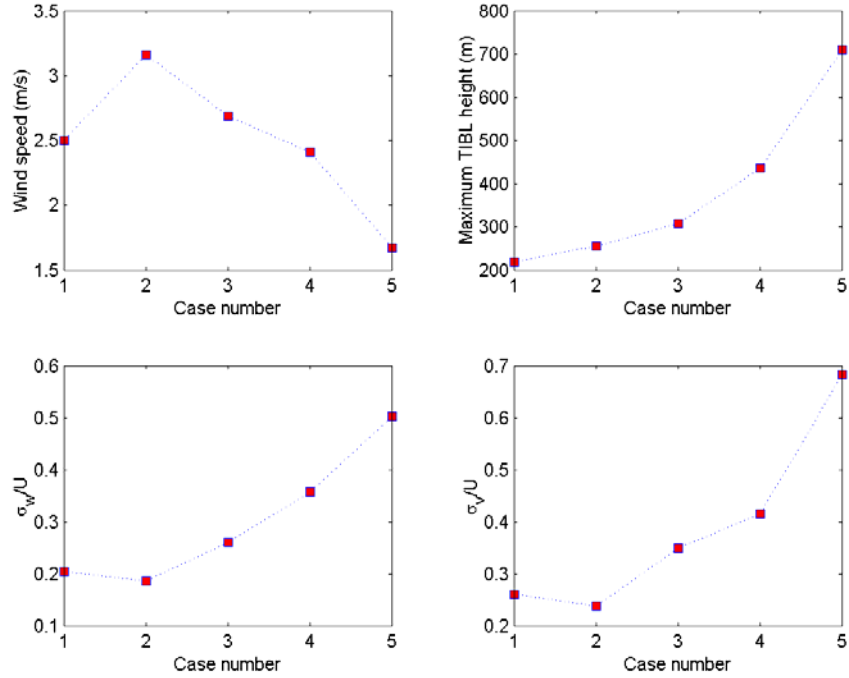


Figure 2.15. Variation of meteorological inputs used to model buoyant releases on 6/27/2005. Case numbers 1 through 5 correspond to hours 7 through 11.

The vertical turbulent intensity within the TIBL, shown in the bottom left panel, increases from about 0.2 at hour 7 to about 0.5 at hour 11. The horizontal turbulent intensity increases from about 0.25 to 0.7 by the end of the experiment.

Figure 2.16 compares observed arc maximum concentrations with model estimates obtained using the inputs depicted in Figure 2.15. Although most of the model estimates are within a factor of two of the observed values, the concentrations are underestimated on the 3 and 5 km arcs.

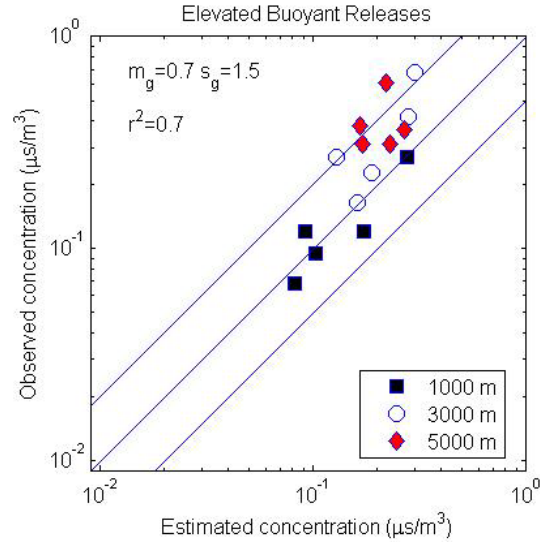


Figure 2.16. Comparison of measured arc maximum concentrations with model results for in-stack releases for the Wilmington 2005 study

Model results improve considerably if the horizontal plume spreads at these distances are decreased by reducing the length scale in Equation (2.4) for σ_y from 2500 m to 1000 m, as seen in Figure 2.17. This is an empirical result, which the research team cannot reasonably justify using at this time.

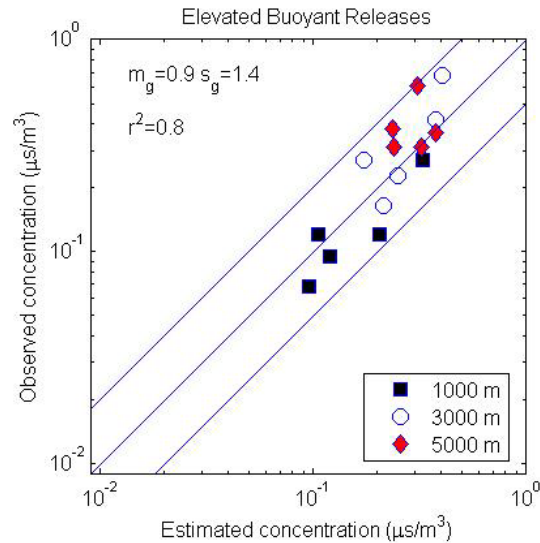


Figure 2.17. Comparison of measured arc maximum concentrations with model results for in-stack releases for the Wilmington 2005 study. $L_y = 1000$ m in Equation (2.4) for horizontal spread.

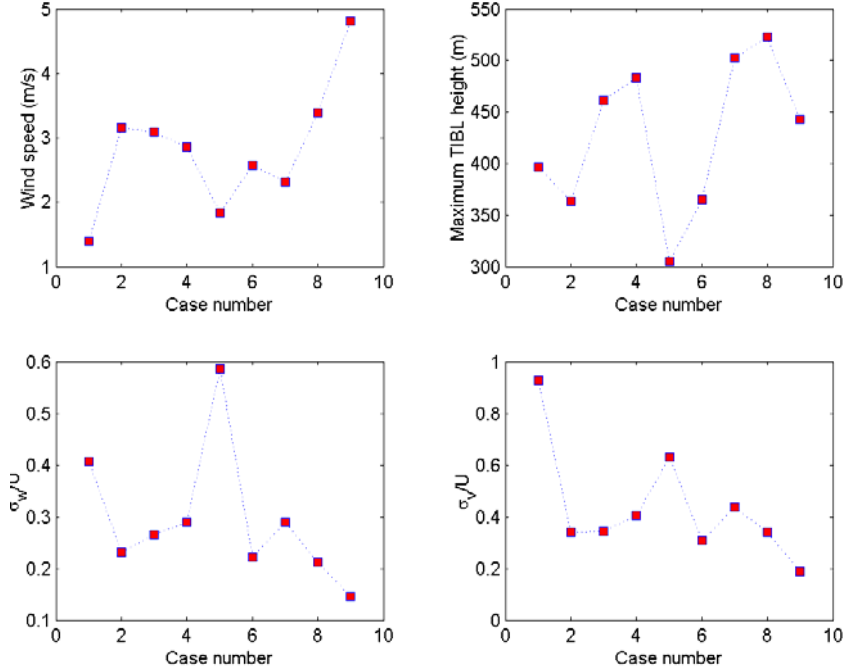


Figure 2.18. Variation of meteorological inputs used to model below stack top releases for the Wilmington 2005 study. Case numbers 1 through 4 correspond to hours 8 through 11 of June 26, while case numbers 5 through 9 refer to hours 7 through 11 of June 28.

Figure 2.18 shows the variation of the inputs used to model the releases below stack top, which occurred during the hours 8 to 11 on June 26, and between hours 7 and 11 on June 28, 2005. Because there were four hours of release on June 26, and 5 hours on June 28, the first four cases refer to the first day, and the remaining to the second day of releases.

The wind speed at 50 m increased from about 1 m/s to just over 3 m/s during the first day. On June 28, the wind speed increased from 2 m/s at hour 7 to close to 5 m/s at hour 11. The maximum TIBL heights range from about 300 m at the start of the experiment to about 500 m by hour 11.

The vertical turbulent intensity within the TIBL, shown in the bottom left panel, lies between 0.2 and 0.4, with one value on June 28 becoming as large as 0.6. The horizontal turbulent intensity ranges from about 0.3 to 0.6 during the two days of the below stack top releases.

Figure 2.19 compares observed arc maximum concentrations with model estimates obtained using the inputs depicted in Figure 2.18. Most of the model estimates are within a factor of two of the observed values, and the model explains 70% of the variance of the observations.

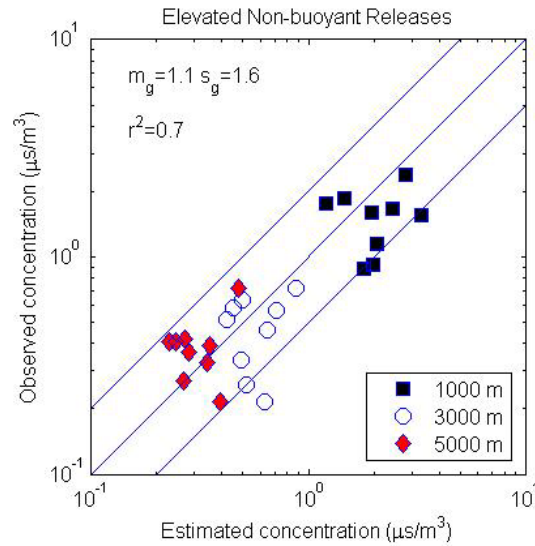


Figure 2.19. Comparison of measured arc maximum concentrations with model results for elevated stack top releases for the Wilmington 2005 study

2.4. Conclusions

The field studies conducted in Wilmington indicates that:

1. Relatively simple dispersion models can be used to estimate ground-level concentrations caused by near-surface sources, such as distributed generation units, or elevated sources, such as power plants. The inputs to these models consist of turbulent and mean velocities averaged over the depth of the thermal internal boundary layer that forms when stable air over water flows onto warmer land.
2. The thermal internal boundary layer (TIBL) plays a crucial role in determining concentrations associated with both surface and elevated releases on the shoreline. Concentrations caused by elevated sources are sensitive to the growth of the TIBL as a function of distance from the shoreline because ground-level concentrations are determined by the entrainment of the plume by the growing TIBL. The TIBL height limits the vertical extent of the plume for surface releases.
3. Commonly used models for the TIBL height, such as that proposed by Venkatram (1977), underestimate the height inferred from ground-level concentrations by as much as a factor of two. In view of the complicated structure of the marine boundary layer that occurs on Los Angeles coastlines (Edinger 1963), this is not surprising. But the TIBL height can be estimated by making empirical corrections to the original formulation.

The dispersion models described here are simple enough to fit readily into the framework of AERMOD, and their inputs are compatible with those required by AERMOD. Details on how the formulation of AERMOD will be modified can be elaborated only when the modifications are implemented. But at this stage, the research team can provide suggestions on how the meteorological inputs required by these models can be generated through the interface between

AERMOD and AERMET. The next section addresses the modifications required in the AERMOD interface.

2.5. Modifications to AERMOD Interface

AERMOD was promulgated as the replacement for the ISC model on November 9, 2005. At this stage, the model cannot be used to estimate the impact of shoreline sources because it does not contain formulations required to account for the interaction between the shoreline TIBL and plumes from near-surface and elevated sources. The major features of the shoreline dispersion models described in this chapter can be readily incorporated into AERMOD to allow its application to an important class of sources. This needs to be followed by evaluation of modified AERMOD with data independent of the Wilmington data set. The data sets collected in the Nanticoke field study (Portelli 1982) and the Kwinana study (Sawford et al. 1998) could be used in this evaluation.

The application of shoreline dispersion models developed in the Wilmington study also requires methods to estimate meteorological inputs from routinely available meteorological observations. AERMET, the meteorological processor for AERMOD (Cimorelli et al. 2005), generates such inputs using routinely available meteorological observations available from the National Weather Service. But AERMET is based on a one-dimensional boundary layer model that cannot be applied to shorelines where surface properties vary sharply across the water-land interface; it is this change in surface properties that produces the thermal internal boundary layer. It will be necessary to modify AERMET or the AERMOD interface to account for these two-dimensional features. The results presented suggest the improvements required in AERMET to make it applicable to shoreline dispersion models.

Because it is not convenient to modify the EPA versions of AERMOD or AERMET, the research team coded the relevant boundary layer equations in AERMET (Cimorelli et al. 2005) and then modified them for application to shorelines. The approach taken here is similar to that in the AERMOD interface (Cimorelli et al. 2005) to account for the TIBL created in the night when stable air from a rural area flows onto the warmer urban surface. The upward heat flux in the urban area is related to the urban-rural temperature difference and the urban TIBL height is related empirically to the urban population. This information is then used to obtain an expression for the convective turbulence generated within the TIBL, which is then added to the turbulence levels generated by AERMET using rural information.

The primary modification required in AERMET (or the AERMOD interface) is including the TIBL height, Equation (2.11), in the model. Then, an expression can be derived for the convectively generated component of turbulence in the TIBL by combining Equations (2.11) and (2.12),

$$\sigma_{wc} = \alpha Q_o^{1/2} \left(\frac{g}{T_o} \right)^{1/3} \left(\frac{2(1+2A)x}{U\gamma} \right)^{1/6}, \quad (2.29)$$

where σ_{wc} (m/s) is added to the shear generated component given by $1.3u_*$ as follows:

$$\sigma_w = (\sigma_{wc}^3 + \sigma_{ws}^3)^{1/3}. \quad (2.30)$$

Note that σ_{wc} depends on the distance from the shoreline, x , but the dependence is weak.

The surface heat flux, Q_o , required to compute the TIBL height is estimated through a surface energy balance over land, included in AERMET. This energy balance is determined by the following inputs: (1) latitude and longitude of Wilmington, (2) surface albedo = 0.2, and (3) the cloud cover fraction = 0.3. The AERMET-based processor uses the information on latitude, surface albedo, and fractional cloudiness to compute net radiation, which is then partitioned between sensible and latent heat flux using the Bowen ratio. The value of γ required in computing the TIBL height can be obtained from routine upper air measurements. This study took $\gamma = 8 \text{ K/1000 m}$, based on temperature measurements at Wilmington.

These inputs used in the calculations are tentative, and are used primarily to illustrate possible methods of estimating meteorological inputs for the shoreline dispersion models developed in this study.

The surface friction velocity is computed by assuming that the mean wind speed well above the urban canopy is known. In practice, this wind speed can be estimated by extrapolating upwards from routinely available surface information, such as that from an airport, and assuming that the wind speed at the chosen level is the same at the urban location. Alternatively, researchers could use an internal boundary layer model, such as that described in Luhar et al. (2006) (See Appendix J) to estimate urban surface parameters from rural measurements.

In this exercise, researchers used the 50 m sodar measurement of the wind speed at the LADWP power plant site. This information was then combined with a z_o of 0.2 m and the heat flux from the surface energy balance to compute the surface friction velocity using similarity wind profiles.

Figure 2.20 compares model estimates of friction velocity and surface heat flux with corresponding observations. The estimated friction velocities agree well with the corresponding observations, but the estimated heat fluxes are generally a factor of two higher than the observations.

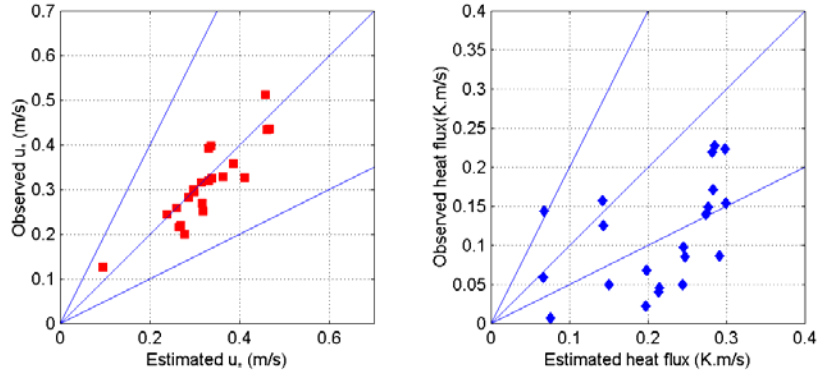


Figure 2.20. Comparison of estimated surface friction velocities and heat fluxes with observations made at LADWP site for the Wilmington 2004 study. The lines above and below the one-to-one correspond to a factor of two interval.

Figure 2.21 compares estimated turbulence levels at the surface and at 50 m with observations made with the sonic anemometer and the sodar. The convective component of the turbulent velocity is evaluated at an effective distance of 100 m from the shoreline. The estimated values of turbulent velocities are within a factor of two of the observations. The agreement between observed and estimated values of σ_v might be fortuitous because the observed values are likely to be controlled by large-scale wind meandering that is not accounted for in the estimates.

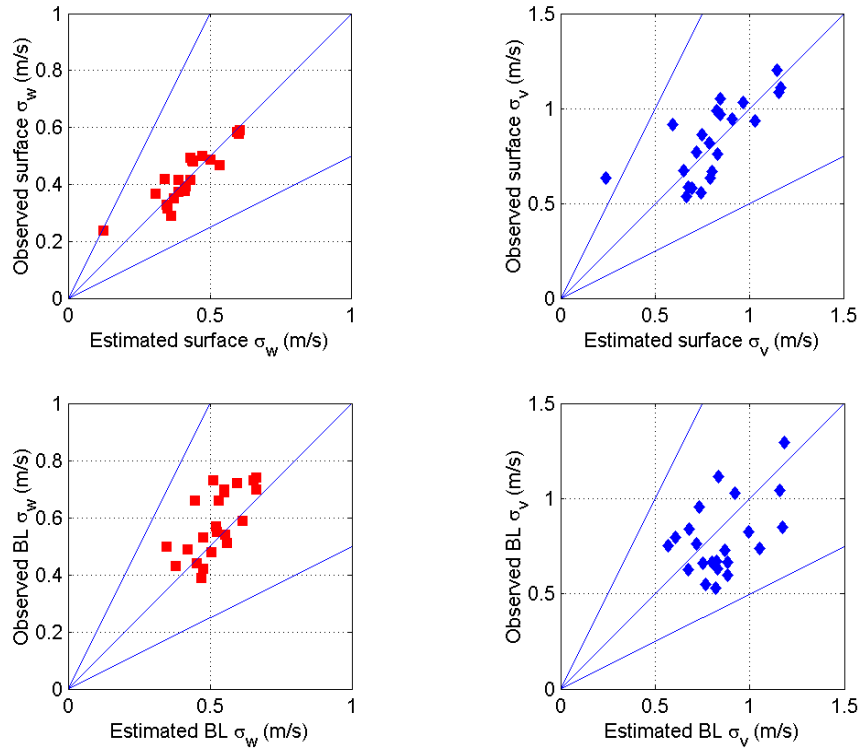


Figure 2.21. Comparison of estimated surface and 50 m (boundary layer, BL) turbulence levels with observations made at the LADWP site for the Wilmington 2004 study. The lines above and below the one-to-one correspond to a factor of two interval.

The left panel of Figure 2.22 compares observations of arc maximum concentrations made during the 2004 field study with model estimates corresponding to the meteorological inputs presented in Figures 2.20 and 2.21. The right panel corresponds to measured meteorological inputs. As indicated earlier, the TIBL heights are calculated by multiplying the result from Equation (2.11) by 2. This is not necessary when the higher estimated heat fluxes are used. A comparison of the results presented in the two panels of the figure shows that model performance using estimated meteorological inputs is comparable to that based on measured inputs.

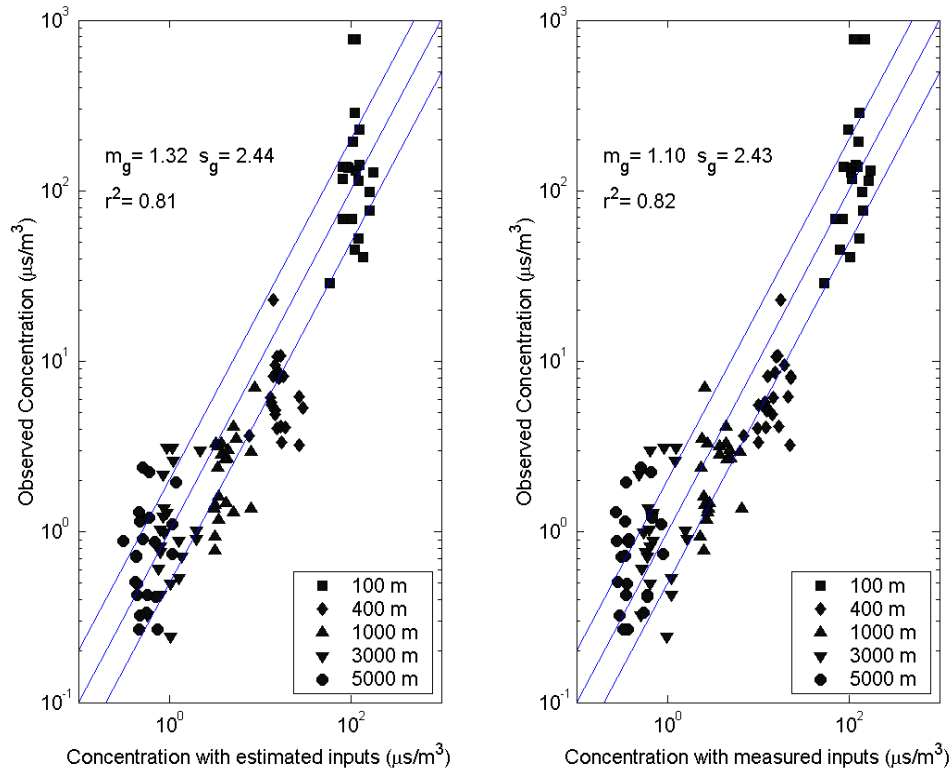


Figure 2.22. Comparison of model results with arc maximum concentrations measured during ground-level releases of the 2004 Wilmington field study

Figure 2.23 illustrates the performance of the dispersion models in explaining the concentrations measured during in-stack releases of 2005 Wilmington study. Figure 2.24 shows the performance of the dispersion model when meteorological inputs are estimated for the cases when releases occurred below stack top. For both buoyant and non-buoyant cases, model performance corresponding to estimates of meteorological inputs is comparable to that obtained using measured inputs (Figures 2.17 and 2.19), except for the 1000 m arc at the second hour of buoyant release, when the model severely underestimates the concentration.

The results presented here suggest that AERMET can be adapted for shoreline applications with relatively simple modifications to account for the contribution of convective turbulence in the shoreline TIBL. The next step is to modify AERMOD and AERMET and evaluate them with several databases.

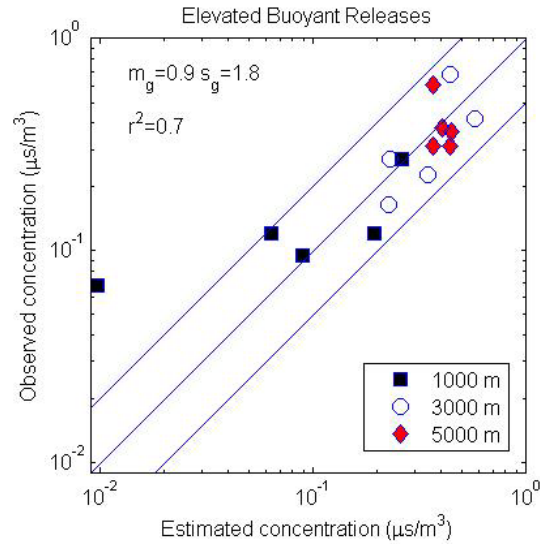


Figure 2.23. Comparison of measured arc maximum concentrations with model results for in-stack releases for the Wilmington 2005 study. Meteorological inputs estimated from 50 m wind speed and Equation (2.30). $L_y = 1000$ m in Equation (2.4) for horizontal spread.

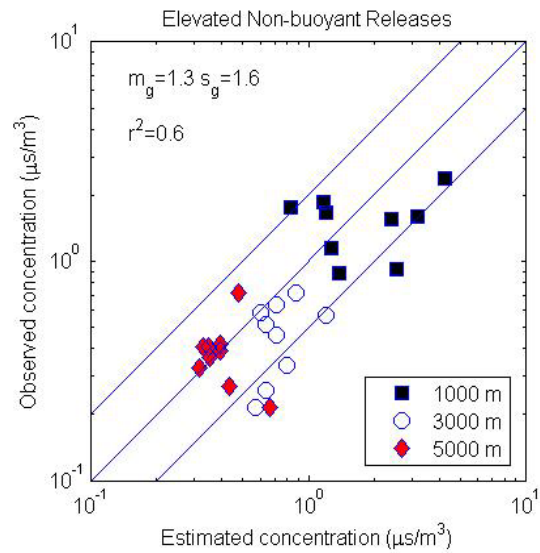


Figure 2.24. Comparison of measured arc maximum concentrations with model results for below stack top releases for the Wilmington 2005 study. Meteorological inputs estimated from 50 m wind speed and Equation (2.30).

3.0 References

- 40 CFR 58 (1987): Code of Federal Regulations: Protection of the Environment, Title 40, Parts 53 to 60.
- Briggs, G. A., 1973: *Diffusion estimation for small emissions*. ERL, ARL USAEC Report ATDL-106, U.S. Atomic Energy Commission, Oak Ridge, Tennessee.
- Cagnetti, P., F. Desiato, P. Gaglione, and A. Pellegrini, 1988: "An Atmospheric Diffusion Study on a Local Scale at a Coastal Site." *Atmospheric Environment* 22, 1051–1059.
- Cimorelli, A. J., S. G. Perry, A. Venkatram, J. C. Weil, R. J. Paine, R. W. Brode, R. B. Wilson, R. F. Lee, W. D. Peters, and R. W. Brode, 2005: "AERMOD: A Dispersion Model for Industrial Source Applications Part I: General Model Formulation and Boundary Layer Characterization." *Journal of Applied Meteorology* 44: 682–693.
- Drivas, P. J., and F. H. Shair, 1974: "A Tracer Study of Pollutant Transport and Dispersion in the Los Angeles Area." *Atmospheric Environment* 8: 1155–1163.
- Edinger, J. G., 1963: "Modification of the Marine Layer over Coastal Southern California." *Journal of Applied Meteorology* 2: 706–712.
- Environmental Protection Agency, 1984: *Quality Assurance Handbook for Air Pollution Measurement Systems. Vol. I, Principles*. EPA Document EPA-600/9-76-005.
- Environmental Protection Agency, 1994: *Quality Assurance Handbook for Air Pollution Measurement Systems, Vol. II: Ambient Air Specific Methods*, EPA Document EPA-600/R-94-038b.
- Environmental Protection Agency, 1989: *Quality Assurance Handbook for Air Pollution Measurement Systems. Vol. IV, Meteorological Measurements*. EPA Document EPA-600/4-82-060.
- Environmental Protection Agency, 1987: *Ambient Monitoring Guidelines for Prevention of Significant Deterioration (PSD)*. EPA Document EPA-450/4-87-007.
- Gamo, M., S. Yamamoto, and O. Yokoyama, 1982: "Airborne Measurements of the Free Convective Internal Boundary Layer during the Sea Breeze." *Journal of Meteorological Society of Japan* 60: 1284-1298.
- Gemmill, D., 2004 : *Improvement of Short Range Dispersion Models to Estimate Air Quality Impact of Power Plants in Urban Environments Quality Assurance Audit Report for Wilmington 2004 Field Study, Revision 1*. Unnumbered UCRCE-CERT Document. September, 1.
- Gemmill, D., 2005 : *Improvement of Short Range Dispersion Models to Estimate Air Quality Impact of Power Plants in Urban Environments: Quality Assurance Audit Report for Wilmington 2005 Field Study*. Unnumbered UCRCE-CERT Document. July, 1.

- Kerman, B. R., R. E. Mickle, R. V. Portelli, N. B. Trivett, and P. K. Misra, 1982: "The Nanticoke Shoreline Diffusion Experiment, June 1978 - II. Internal Boundary Layer Structure." *Atmospheric Environment* 16: 423–437.
- Lamb, B. K., A. Lorenzen, and F. H. Shair, 1978a: "Atmospheric Dispersion and Transport within Coastal Regions – Part I. Tracer Study of Power Plant Emissions from the Oxnard Plain." *Atmospheric Environment* 12: 2089–2100.
- Lamb, B. K., F. H. Shair, and T. B. Smith, 1978b: "Atmospheric Dispersion and Transport within Coastal Regions – Part II. Tracer Study of Industrial Emissions in the California Delta Region." *Atmospheric Environment* 12: 2101–2118.
- Luhar, A. K., 1998: "An Analytical Slab Model for the Growth of the Coastal Thermal Internal Boundary Layer under near-Neutral Onshore Flow Conditions." *Boundary-Layer Meteorology* 88: 103–120.
- Luhar, A. K., 2002: "The Influence of Vertical Wind Direction Shear on Dispersion in the Convective Boundary Layer, and its Incorporation in Coastal Fumigation Models." *Boundary-Layer Meteorology* 102: 1–38.
- Luhar, A. K., A. Venkatram, Sang-Mi Lee, 2006: On Relationship between Urban and Rural Surface Meteorology for Diffusion Applications, to appear in *Atmospheric Environment*.
- McElroy, J. L., and F. Pooler, 1968: *The St. Louis dispersion study Volume II - analysis*. National Air Pollution Control Administration, Pub. No. AP-53, US DHEW Arlington, 50 pp.
- Misra, P. K., 1980: "Dispersion from Tall Stacks into a Shore Line." *Atmospheric Environment* 14: 397–400.
- Misra, P. K., and S. Onlock, 1982: Modelling Continuous Fumigation of Nanticoke Generating Station Plume. *Atmospheric Environment* 16: 479–489.
- Murray, D. R., and N. E. Bowne, 1988: *Urban Power Plant Plume Studies*. EPRI Report No. EA-5468, Research Project 2736-1, Electric Power Research Institute, Palo Alto, California.
- Ogawa, Y., T. Ohara, S. Wakamatsu, P. G. Diosey, and I. Uno, 1986: "Observation of Lake Breeze Penetration and Subsequent Development of the Thermal Internal Boundary Layer for the Nanticoke II Shoreline Diffusion Experiment." *Boundary-Layer Meteorology* 35: 207–230.
- Portelli, R. V., 1982: "The Nanticoke shoreline diffusion experiment, June 1978 - I. Experimental design and program overview." *Atmospheric Environment* 16: 413–421.
- Rotach, M. W., 1993: "Turbulence Close to a Rough Urban Surface Part 1: Reynolds Stress." *Boundary-Layer Meteorology* 65: 1–28.

- Sawford, B. L., A. K. Luhar, J. M. Hacker, S. A. Young, I.-H. Yoon, J. A. Noonan, J. N. Carras, D. J. Williams, and K. N. Rayner, 1998: "The Kwinana Coastal Fumigation Study: I - Program Overview, Experimental Design and Selected Results." *Boundary-Layer Meteorology* 89: 359–384.
- Shair, F. H., E. J. Sasaki, D. E. Carlan, G. R. Cass, W. R. Goodin, J. G. Edinger, and G. E. Schacher, 1982: "Transport and Dispersion of Airborne Pollutants Associated with the Land Breeze-Sea Breeze System." *Atmospheric Environment* 16: 2043–2053.
- Stull, R. B., 1988: *An Introduction to Boundary Layer Meteorology*. Kluwer Academic Publishers, Dordrecht. 666 pp.
- Stunder, M., and S. Sethuraman, 1986: "A Statistical Evaluation and Comparison of Coastal Point Source Dispersion Models." *Atmospheric Environment* 20: 301–315.
- Van Dop, H., R. Steenkist, and F. T. M. Nieuwstadt, 1979: "Revised Estimates for Continuous Shoreline Fumigation." *Journal of Applied Meteorology* 18: 133–137.
- Venkatram, A., 1977: "A Model of Internal Boundary-layer Development." *Boundary-Layer Meteorology* 11: 419–437.
- Venkatram, A., 2003: Improvement of Short Range Dispersion Models to Estimate Air Quality Impact of Power Plants in Urban Environments: Measurement Report for Technical Support Study. UCR ME Document UCR/ME-RPP4-2. December 5.
- Venkatram, A., 2004: Improvement of Short Range Dispersion Models to Estimate Short Range Impact of Power Plants in Urban Environments: Work Plan for Main Field Study. UCR ME Document UCR/ME-RPP4-3. May 21.
- Venkatram, A., V. Isakov, D. Pankratz, and J. Yuan, 2005: "Relating Plume Spread to Meteorology and Urban Areas." *Atmospheric Environment* 39: 371–380.
- Yuan, J., A. Venkatram, and V. Isakov, 2006: "Dispersion from Ground-level Sources in a Shoreline Urban Area." *Atmospheric Environment* 40: 1361–1372.

4.0 Glossary

AERMET	AERMOD's meteorological processor
AERMOD	A steady-state plume model
ARB	California Air Resources Board
BL	boundary layer
CSIRO	Commonwealth Scientific and Industrial Research Organization
g/sec	grams per second
GC	gas chromatographs
Hz	Hertz
ISC	Industrial Source Complex model
JWPCP	Los Angeles County Sanitation Districts' Joint Water Pollution Control Plant
kg/hr	kilograms per hour
K	kelvin
LADWP	Los Angeles Department of Water & Power
Lidar	<u>L</u> ight <u>D</u> etection <u>A</u> nd <u>R</u> anging
L/min	liters per minute
m/s	meters per second
PVC	polyvinyl chloride
SF ₆	sulfur hexafluoride
SO ₂	sulfur dioxide
TIBL	thermal internal boundary layer
TSS	technical support study
UCR	University of California, Riverside
μs/m ³	microsecond per cubic meter
USEPA	U.S. Environmental Protection Agency

Appendices

These appendices are available in a separate document.

- Appendix A** Measurement Report for Technical Support Study of the Wilmington Field Study
- Appendix B** Tracer Release System Failure
- Appendix C** Measurements and Data Processing for the Wilmington 2004 Field Study
- Appendix D** Quality Assurance Audit Report for the Wilmington 2004 Field Study
- Appendix E** Wind Data Summary and Wind Roses for the Wilmington 2004 Field Study
- Appendix F** Tracer Release and Sampling Details for the Wilmington 2004 Field Study
- Appendix G** Measurements and Data Processing for the Wilmington 2005 Field Study
- Appendix H** Quality Assurance Audit Report for the Wilmington 2005 Field Study
- Appendix I** Key to Electronic Data Files
- Appendix J** Estimating Micrometeorological Inputs for Modeling Dispersion in Urban Areas During Stable Conditions